



## Exploring the molecular mechanism of Yinao Fujian formula on ischemic stroke based on network pharmacology and experimental verification

Jing Lu <sup>a,1</sup>, Xiaolei Tang <sup>a,1</sup>, Yuxin Zhang <sup>a</sup>, Hongbo Chu <sup>a</sup>, Chenxu Jing <sup>a</sup>,  
Yufeng Wang <sup>b</sup>, Huijuan Lou <sup>b</sup>, Ziqi Zhu <sup>c</sup>, Daqing Zhao <sup>d</sup>, Liwei Sun <sup>a,\*</sup>,  
Deyu Cong <sup>b,\*\*</sup>

<sup>a</sup> Research Center of Traditional Chinese Medicine, The Affiliated Hospital to Changchun University of Chinese Medicine, Jilin, China

<sup>b</sup> Department of Tuina, The Affiliated Hospital to Changchun University of Chinese Medicine, Jilin, China

<sup>c</sup> College of Acupuncture and Tuina, Changchun University of Chinese Medicine, Jilin, China

<sup>d</sup> Jilin Ginseng Academy, Changchun University of Chinese Medicine, Jilin, China

### ARTICLE INFO

#### Keywords:

Ischemic stroke  
Yinao Fujian formula  
Network pharmacology  
Oxidative stress  
Inflammation

### ABSTRACT

**Background:** Ischemic stroke (IS) is a leading cause of long-term disability and even mortality, threatening people's lives. Yinao Fujian (YNFJ) formula is a Traditional Chinese Medicine formula that has been widely used to treat patients with IS. However, the molecular mechanism of YNFJ for the treatment of IS is still elusive. Our study aimed to explore the potential protective effect and the underlying mechanisms of YNFJ on IS using a network pharmacology approach coupled with experimental validation.

**Materials and methods:** Effective compounds of YNFJ were collected from BATMAN-TCM and TCMSD databases, while IS targets were obtained from GeneCards, OMIM, TTD and DrugBank databases. The protein-protein interaction (PPI) network was constructed to further screen the hub targets of YNFJ in IS treatment. GO and KEGG enrichment analyses were used to identify the critical biological processes and signaling pathways of YNFJ for IS. Moreover, Nissl staining, HE, TTC staining and Tunel staining were used in the MCAO model to prove the neuroprotective effect of YNFJ. Oxidative damage, inflammatory factor release and related pathways were tested in MCAO rat model and hypoxia-induced BV2 cell model, respectively.

**Results:** We found that YNFJ treatment significantly alleviated MCAO-induced nerve damage and apoptosis. Then, network pharmacology screening combined with literature research revealed IL6, TNF, PTGS2, NFKBIA and NFE2L2 as the critical targets in a PPI network. Moreover, the top 20 signaling pathways and biological processes associated with the protective effects of YNFJ on IS were enriched through GO and KEGG analyses. Further analysis indicated that NF- $\kappa$ B and Nrf2/HO-1 signaling pathways might be highly involved in the protective effects of YNFJ on IS. Finally, *in vitro* and *in vivo* experiments confirmed that YNFJ inhibited the release of inflammatory factors (IL-6 and TNF- $\alpha$ ) and MDA content, and increased the activity of SOD. In terms of the mechanism, YNFJ inhibited the release of inflammatory factors by suppressing the NF- $\kappa$ B pathway and decreased the expression of iNOS and COX-2 to protect microglia from inflammation damage. In

\* Corresponding author.

\*\* Corresponding author.

E-mail addresses: [Sunyililwei@163.com](mailto:Sunyililwei@163.com) (L. Sun), [congdeyu666@sina.com](mailto:congdeyu666@sina.com) (D. Cong).

<sup>1</sup> These authors have contributed equally to this work and share the first authorship.

<https://doi.org/10.1016/j.heliyon.2023.e23742>

Received 17 April 2023; Received in revised form 17 October 2023; Accepted 12 December 2023

Available online 16 December 2023

2405-8440/© 2023 Published by Elsevier Ltd.

This is an open access article under the CC BY-NC-ND license

(<http://creativecommons.org/licenses/by-nc-nd/4.0/>).

addition, YNFJ initiated the dissociation of Keap-1 and Nrf2, and activated the downstream protein HO-1, NQO1, thus decreasing oxidative stress.

**Conclusion:** Taken together, the findings in our research showed that the protective effects of YNFJ on IS were mainly achieved by regulating the NF- $\kappa$ B and Nrf2/HO-1 signaling pathways to inhibit oxidative stress damage and inflammatory damage of microglia.

## 1. Introduction

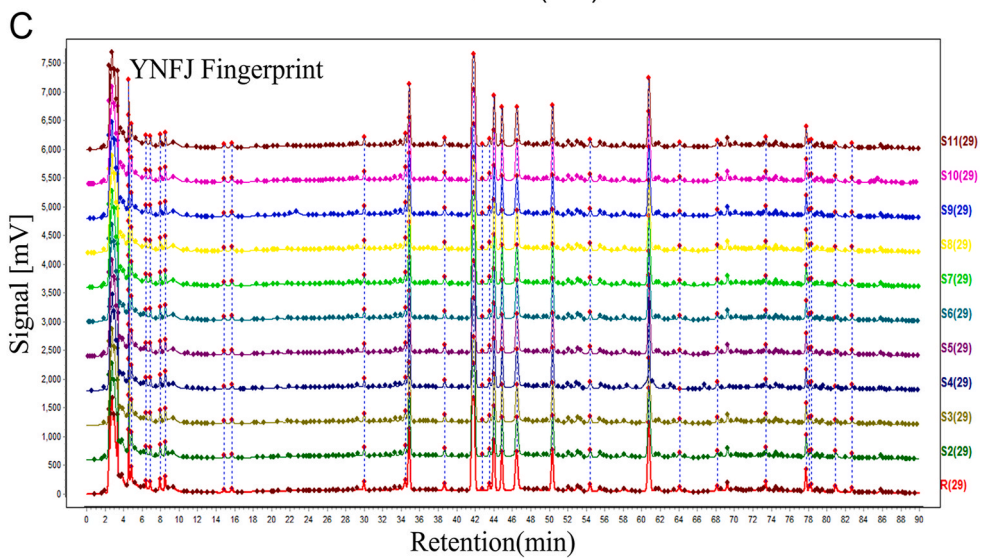
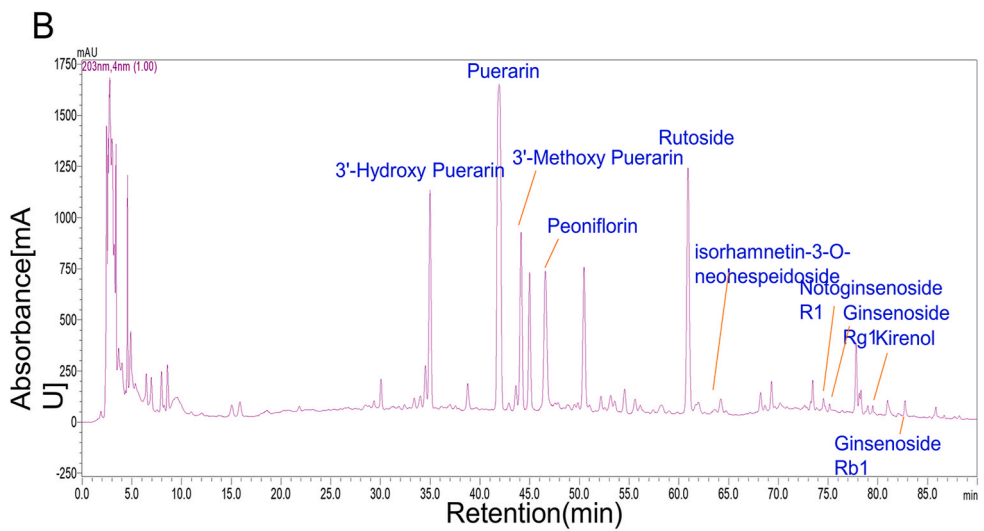
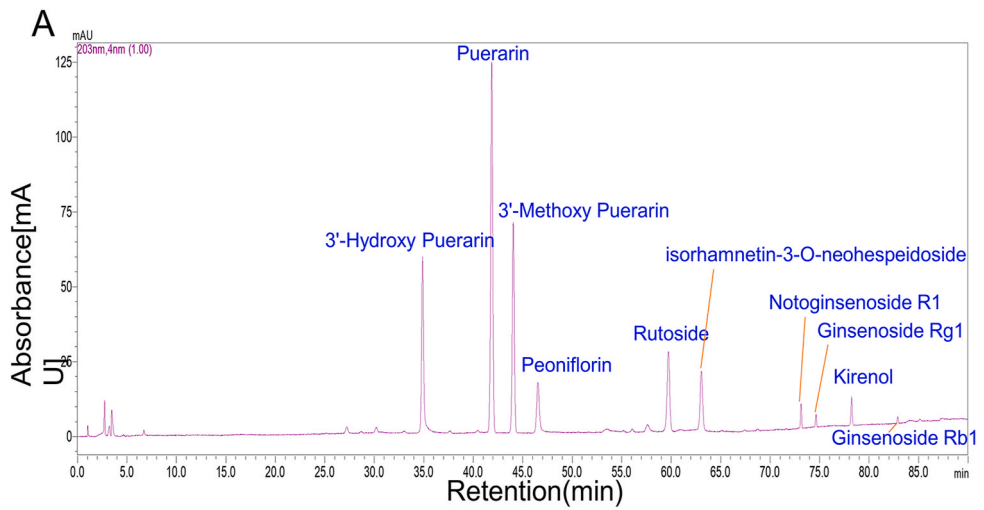
Ischemic stroke is an acute cerebrovascular disease caused by thrombosis or occlusion of the cerebral arteries. Studies have shown that ischemic stroke has become one of the most common causes of death and disability worldwide, placing a heavy burden on society and economy (<https://www.who.int>). Despite numerous clinical trials of therapeutics, current treatment options are still limited to the use of anticoagulants, as well as thrombolysis and mechanical recanalization. Therefore, there is an urgent need for novel safe and affordable adjuvant treatment strategies.

Traditional Chinese Medicine (TCM) is expert in combining the efficacy of different Chinese medicines to treat various diseases, including ischemic stroke. As compared with Western medicine, TCM has fewer adverse effects as well as a more systematic influence on pharmacological activity and efficacy. Currently, discovering proven therapeutic drugs for ischemic stroke has become an important challenge. Yinao Fujian (YNFJ) Formula is a good prescription beneficial for ameliorating ischemic stroke, created by Chinese Medical Master Jixue Ren, who has 65 years of medical experience in China. Professor Ren proposed that blood stasis is an important cause of stroke and a key factor in poor prognosis. Based on this, Professor Ren proposed to use the YNFJ to treat ischemic stroke, which has been used as an in-hospital preparation (named Chuanhong Zhongfeng Capsule) for more than 30 years, and has won multiple awards including the National Science and Technology Progress Award of China. The clinical retrospective study results of 352 cases of YNFJ showed that YNFJ can effectively reduce the recurrence rate, promote the recovery of neurological function, reduce the degree of disability, and improve daily living ability [1–4]. Our previous work has indicated that YNFJ had great pharmacology efficacy on IS by *in vivo* and *in vitro* experiments, and its mechanism of action is related to Nrf2-mediated neuroinflammation [5]. YNFJ is composed of Paeoniae Radix Rubra, Chuanxiong Rhizoma, Typhae Pollen, Puerariae Lobatae Radix, Sophorae Flos, Carthami Flos, Siegesbeckiae Herba, Notoginseng Radix Et Rhizoma. Moreover, some studies have shown that the active ingredient of YNFJ has anti-inflammatory and antioxidant effects. For example, paeoniflorin [6], Puerarin [7], Hydroxysafflor Yellow A [8] and *Panax notoginseng saponins* [9], etc. all have the effect of inhibiting neuroinflammation after brain injury. In addition, Chuanxiong extract [10], Hydroxysafflor Yellow A [11], and various *Panax notoginseng saponins* [12] have protective effects on nerve cells from oxidative damage. Therefore, we speculate that YNFJ may exert neuroprotective effects through anti-inflammatory and antioxidant effects. Nevertheless, the underlying effects and potential molecular mechanism of the neuroprotective effects of YNFJ for treating ischemia remain elusive.

Network pharmacology is an emerging discipline that reveals the regulatory effect of TCM on the body network, which can be used to screen the molecular targets of Chinese herbs and Traditional Chinese Medicine formulas, and predicts their signaling pathways and mechanisms of action [13]. Hence, this experiment investigated the possible molecular mechanisms of YNFJ to alleviate ischemic stroke-induced CNS injury via network pharmacology and experimental verification.

**Table 1**  
The compositions of the Yinao Fujian (YNFJ) formula.

Chinese name	English name	Latin name	Family	Part used	Proportion	Voucher specimen
Chi Shao	Paeoniae Radix Rubra	<i>Paeonia lactiflora</i> Pall.	Paeoniaceae	Root	2	190,208–1
Chuan Xiong	Chuanxiong Rhizoma	<i>Ligusticum chuanxiong</i> Hort.	Umbelliferae	Rhizome	1	190,317–1
Pu Huang	Typhae Pollen	<i>Typha orientalis</i> C.Presl	Typhaceae	Pollen	1.5	190,317–2
Ge Gen	Puerariae Lobatae Radix	<i>Pueraria montana</i> var. <i>lobata</i> (Willd.) Sanjappa & Pradeep	Fabaceae	Root	3	190,319–1
Huai Hua	Sophorae Flos	<i>Styphnolobium japonicum</i> (L.) Schott	Fabaceae	Flower	1	190,321–1
Hong Hua	Carthami Flos	<i>Carthamus tinctorius</i> L.	Asteraceae	Flower	2	190,321–2
Xi Xiancao	Siegesbeckiae Herba	<i>gesbeckia pubescens</i> (Makino) Makino	Asteraceae	Aerial parts	2	190,321–3
San Qi	Notoginseng Radix Et Rhizoma	<i>Panax notoginseng</i> (Burkill) F-H.Chen	Araliaceae	Root	3	190,321–4
Di Long	Pheretima	<i>Pheretima aspergillum</i> (E. Perrier) or <i>Pheretima vulgaris</i> Chen or <i>Pheretima guillelmi</i> (Michaelsen) or <i>Pheretima pectinifera</i> Mkhakeen	Megascolecidae	Whole body	1	190,321–5



(caption on next page)

**Fig. 1.** High Performance Liquid Chromatography (HPLC) analysis of YNFJ. (A) HPLC Chromatogram of mixed standards, including 3'-Hydroxy Puerarin, Puerarin, 3'-Methoxy Puerarin, Peoniflorin, Rutoside, isorhamnetin-3-O-neohespeidoside, Notoginsenoside R1, Ginsenoside Rg1, Kirenol and Ginsenoside Rb1 at 203 nm. (B) HPLC chromatogram of YNFJ at 203 nm. (C) HPLC fingerprint chromatograms of 10 batches of TNFJ (S1–10) from the analysis of 10 batches of YNFJ at 203 nm.

## 2. Materials and methods

### 2.1. .1. Preparation of YNFJ extract

YNFJ contains 9 different Chinese medicinal materials, all of which were purchased from the Department of Pharmacy in our hospital. The components of YNFJ were Chi Shao, Chuan Xiong, Pu Huang, Ge Gen, Huai Hua, Hong Hua, Xi Qiancao, San Qi and Di Long (Table 1). The compound was processed based on the standard procedures of the Chinese Pharmacopoeia [14]. Briefly, soak the mixed compound with 10 times the volume of water, and extract at 100 °C for 30 min. Repeat the extraction 3 times and mix the extracts together. After filtration and centrifugation, the supernatant is concentrated and frozen in a vacuum to obtain a brownish powder. Finally, we obtained the yielded percentage of the experimental powder of 18.52 %.

### 2.2. HPLC analysis

The standard spectrum of YNFJ HPLC was detected using the High-performance liquid chromatography (HPLC) and diode array detector (DAD) [15]. The mobile phase component is an acetonitrile aqueous solution and 0.4 % phosphoric acid aqueous solution mixture. A detected wavelength of 203 nm was used to obtain the chromatographic separation. The standard mixed with 3'-Hydroxy Puerarin, Puerarin, 3'-Methoxy Puerarin, Paeoniflorin, Rutoside, isorhamnetin-3-O-neohespeidoside, Notoginsenoside R1, Ginsenoside Rg1, Kirenol and Ginsenoside Rb1 was used as a control to analyze retention time (Fig. 1A). By comparing the retention time with standards, ten peaks of YNFJ were determined (Fig. 1B). The similarities were found to be > 90 % for all 10 batches analyzed, implying a relatively well overall quality and reproducibility of YNFJ (Fig. 1C).

### 2.3. Network pharmacology analysis

#### 2.3.1. Establishment of the ingredient-target network between YNFJ and ischaemic stroke

Network pharmacology analysis was completed according to standard procedures recommended by Li's team [16]. Briefly, effective compounds of YNFJ ( Huaihua, Honghua, Gegen, Xixiancao, Puhuang, Chuanxiong, Chishao, Dilong, Sanqi ) were collected from BATMAN-TCM (<http://bionet.ncpsb.org/batman-tcm/>) and TCMSP (<https://tcmsp-e.com/tcmsp.php>) databases, using the parameters of drug-likeness (DL) and oral bioavailability (OB). The screening conditions for effective compounds of YNFJ were  $DL \geq 0.18$  and  $OB \geq 30\%$ . Apply the SwissTargetPrediction database to predict the potential target protein of YNFJ. After removing the duplicate values, the potential target protein of YNFJ was obtained, and then convert the gene name through the UniProt database. Disease targets were identified from four databases, named GeneCards, OMIM, TTD, and DrugBank databases using "Ischemic stroke" as the search term. The screening criteria for the GeneCards database are the median of the target correlation score. After merging four databases and removing duplicates, the UniProt database is used for standardization to ultimately obtain potential targets for ischemic stroke. Moreover, with the help of R 4.1.3, a Venn diagram was drawn to demonstrate the common target of YNFJ and ischemic stroke. Finally, we established the interaction network between YNFJ ingredient and ischemic stroke targets using Gephi 0.9.2 software.

#### 2.3.2. Establishment of protein-protein interaction (PPI) network

The typical targets of YNFJ and IS are screened out by Venny's diagram. The common targets were analyzed using the STRING database (<https://string-db.org/>), with the species limited to Homo sapiens, completing the protein-protein interaction (PPI) network. In Cytoscape 3.9.1, CytoNCA was used to continue numerical calculation, and evaluate the topological characteristics of each node in combination with parameters such as Local Average Connectivity-based, Eigenvector Centrality, Betweenness Centrality, Network Centrality, Degree Centrality and Closeness Centrality. The median values of all parameter indicators were calculated using R screening. Genes > median were identified as the hubgenes.

### 2.4. Pathway enrichment analyses

We used the omicshare platform (<https://www.omicshare.com/>) to finish the Kyoto Encyclopedia of Genes and Genomes (KEGG) and Gene ontology (GO) enrichment analysis of common target genes.

### 2.5. Animal model construction

The research was conducted in accordance with the internationally accepted principles for laboratory animal use and care in the European Community guidelines (EEC Directive of 1986; 86/609/EEC), and was approved by the Experimental Animal Committee of Changchun University of Chinese Medicine (NO. 2020143). Totally, 60 adult male Sprague-Dawley (SD) rats (8–10 weeks, bodyweight 270–320 g), provided by the Animal Center of Yisi (Changchun, China), were raised in the SPF-level laboratory Animal Room. Animals

were housed in a specific pathogen-free (SPF) animal room on a 12 h circadian cycle, which was reared at 45%–55% relative humidity and  $22 \pm 2$  °C with enough food and water. 60 rats were randomly separated into 3 experimental groups: sham ( $n = 20$ ), MCAO ( $n = 20$ ), and MCAO + YNFJ ( $n = 20$ ). As previously described, MCAO was introduced to induce focal cerebral ischemia [17]. Firstly, the right common carotid artery was exposed and the external carotid artery was cut. Secondly, a ligature was applied for 2 h by passing a monofilament (0.26 mm in diameter) with a rounded tip through the right external carotid artery and into the middle carotid artery. Then the suture was slowly withdrawn for reperfusion body temperature was monitored with a thermostatically controlled heating blanket to maintain the temperature at  $37.0 \pm 0.5$  °C. Sham surgery rats were subjected to the same surgical procedures except that the monofilament was not advanced into the middle carotid artery. A laser Doppler flowmeter was used to measure the ipsilateral cerebral blood flow. If the cerebral blood flow decreased more than 80% of the baseline during occlusion, we considered the MCAO model was successfully constructed. On the next day after establishing the MCAO model, different doses of YNFJ (0.82 g/kg) were intragastrically administered to the rats. In our pre-experiment, the effects of YNFJ at different doses of 0.21, 0.41, 0.82 and 1.64 g/kg were evaluated by IL-6 and MDA analysis. The results proved a most significant reduction of IL-6 and MDA after treatment with 0.82 g/kg YNFJ in rats, which indicated a significant therapeutic effect (Fig. 2A and B). Therefore, we selected the concentration with the best therapeutic effect (0.82 g/kg) for the following animal experiments.

## 2.6. Cell model construction

Mouse microglial cells (BV2 cell line) were cultured in MEM (Gibco, Life technologies, USA) mixed with 10% FBS, penicillin (100 U/mL), and streptomycin (100  $\mu$ g/mL) at 37 °C in with 5% CO<sub>2</sub>. To establish hypoxia-disposed cell injury models, BV2 cells were cultured in BioSpa automated incubator with the condition of 1%O<sub>2</sub>, 94% N<sub>2</sub>, 5% CO<sub>2</sub> for 12 h, which activated the inflammatory response and oxidative stress of BV2 cells.

## 2.7. TTC staining

We performed TTC staining to assess the infarct volume of brain tissues in tested rats. Briefly, brain tissues isolated from rats were frozen at  $-20$  °C for 20 min and then cut into 5 sections (2-mm) in the coronal plane at the level of the optic chiasm. Afterward, we chose 2% TTC phosphoric acid buffer to treat the obtained sections, followed by incubation at 37 °C darkly for 30 min. After staining using TTC, the normal brain tissues were observed as red, while the infarct loci were red as white. The digital camera (Canon SX20; Canon, Inc., Tokyo, Japan) was introduced to capture images, and ImageJ (Bethesda, MD, USA) was adopted to calculate the percentage of the IV in the total brain volume [18].

## 2.8. Hematoxylin and Eosin (HE) staining

As previously described, the tissue sections were firstly embedded in paraffin, afterward, they were deparaffinized in a conventional gradient, and then HE stained at 25 °C for 3 min. After rinsing with running water, the tissue sections were placed into a 75% alcohol/hydrochloric acid mixture for 30 s. Then, the sections were washed with running water until they turned back to blue. Then, the tissue sections were continuously treated with 95% ethanol, and stained in acidified eosin-ethanol for 1 min. Finally, tissue sections were treated with graded ethanol and xylene to make the slice transparent. Then treated with neutral balsam to obtain HE-stained sections [19]. Tissues were observed under an optical microscope (Canon SX20) to determine the morphological changes.

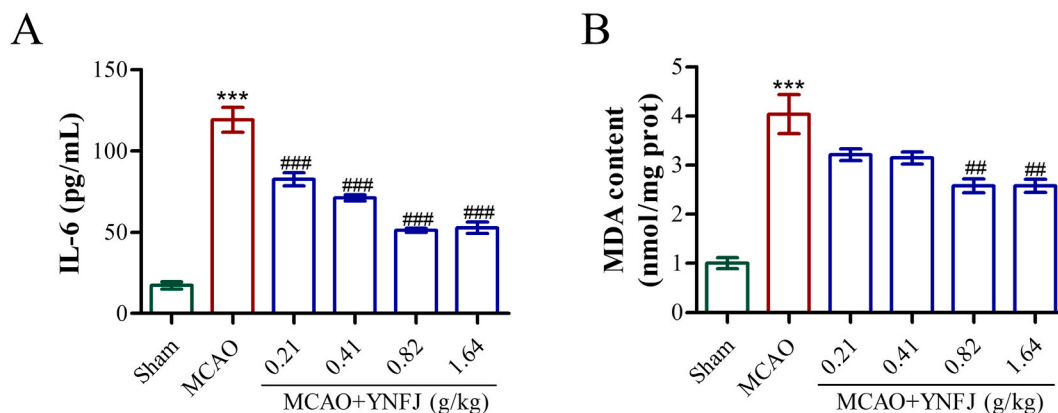


**Fig. 2.** The effect of different doses of YNFJ on MCAO rats. (A) The level of IL-6 was assessed by ELISA. (B) A representative histogram of MDA content in ischemic penumbra of MCAO rats. \*\*\* $p < 0.001$  vs. sham group; ## $p < 0.01$ , ### $p < 0.001$  vs. MCAO model group.  $n = 3$  per group.

## 2.9. Nissl staining

Nissl staining was carried out the experimental procedures in strict accordance with the manufacturer's manual. Briefly, slices were deparaffinized using different concentrations of xylene and alcohol solutions. Then, slices were stained in nissl staining solution for 5 min at 37 °C. After slices were washed twice with PBS, they were dehydrated with 95 % ethanol solution, and transparent with xylene solution [20]. We counted the number of Nissl-positive neurons in the penumbra by an optical microscope (Canon SX20). And each of the tissue sections was viewed in 5 random fields.

## 2.10. Tunel assay

We performed the Tunel assay to observe the apoptotic condition of tissues under cryosections. Briefly, Soak the prepared frozen slices in Tunel staining solution and incubate for 1 h under dark conditions at 37 °C. After that, the nucleus was stabilized by DAPI. Wash the slices with PBS three times to clean the excess staining solution. Among which, sections were observed with a confocal microscope (Nikon, Tokyo, Japan) [21].

## 2.11. Superoxide dismutase (SOD) and malondialdehyde (MDA) analysis

The cell sourced or tissue sourced levels of SOD and MDA were detected using the corresponding SOD and MDA kits. First, the cold RIPA lysis buffer was added to the tissue or cells, then centrifuged at 10,000 rpm/min for 10 min. Afterward, we collected the supernatant to measure the levels of SOD and MDA.

For SOD detection, 100  $\mu$ L sample preparation solution was added with  $1 \times 10^6$  cells. Lysed cells were centrifuged at 12,000 g for 5 min at 4 °C. After that, fully mixed 20  $\mu$ L supernatant or standards and 160  $\mu$ L enzyme working solution with 20  $\mu$ L reaction starting liquid, followed by detecting at an absorbance value of 450 nm.

For MDA detection, add 200  $\mu$ L DMA solution to 100  $\mu$ L sample preparation solution, 100 °C water bath for 15 min. After cooling to room temperature, centrifuge 1000g for 10 min. Add 200  $\mu$ L supernatant to a 96 well plate and set the absorbance value parameter to 532 nm for detection. Bring the test results into the standard curve to obtain the MDA content, and divide it by the protein concentration to obtain the MDA content. Protein concentration was an internal control [22].

## 2.12. Enzyme-linked immunosorbent assay (ELISA)

ELISA assay was administrated to evaluate the inflammatory factors in cells according to the Manufacturer instructions. ELISA kits of IL-6 and TNF- $\alpha$  were obtained from R&D Systems (Minneapolis, MN, USA). The rat brain tissue homogenate or cell medium supernatant was centrifuged at 50,00 $\times$ g and 4 °C for 10 min. And the supernatant was collected. 100  $\mu$ L Standard control or supernatant was added separately into the well of coated plate, and incubated at 37 °C for 1 h. Afterward, 100  $\mu$ L biotin-antibody was added and incubated at 37 °C for another 1 h. After washing the plate with washing buffer for 3 times, 100  $\mu$ L streptavidin-HRP and 90  $\mu$ L TMB substrate were incubated at 37 °C for 15 min, respectively. Finally, added 50  $\mu$ L stopping solution to stop the reaction. The absorbance was measured in a microplate reader at 450 nm.

## 2.13. Western blotting

The concentration of the tissues or cells protein was tested by BCA kit (Invitrogen). Totally, 40  $\mu$ g/sample were separated by 12 % SDS-PAGE, and transferred to a polyvinylidene fluoride (PVDF) membrane. After blocked with 5 % BSA at room temperature for 1 h, the membranes were mixed with the primary antibodies (1:1000) overnight at 4 °C. Then, membrane was mixed with the secondary antibodies with horseradish peroxidase (with the dilution of 1:5000) for 30 min. FluorChem Imager System (ProteinSimple, San Jose, CA, USA) was adopted to visualize the protein band and the gray value for each band was calculated using AlphaView Software (ProteinSimple) [23,24]. Antibodies against Nrf2 (110 kDa, ab137550), NQO1 (31 kDa, ab80588), I $\kappa$ B $\alpha$  (39 kDa, ab32518), iNOS (140 kDa, ab136918), GAPDH (37 kDa, #5174), COX2 (69 kDa, ab179800), CD68 (37 kDa, ab201340) were purchased from Abcam (Cambridge). Antibodies against p-p65 (65 kDa, #3033), p65 (65 kDa, #8242), p-I $\kappa$ B $\alpha$  (40 kDa, #5209), Keap-1 (60–64 kDa, #8047), HO-1 (28 kDa, #43966) were obtained from Cell Signaling Technology (Beverly, MA, USA).

## 2.14. Immunofluorescence staining

The prepared paraffin sections were subjected to deparaffinization, rehydration and antigen retrieval treatments. Then the sections were quenched with 0.3 % hydrogen peroxide and blocked with BSA for 1 h at room temperature. Different antibodies (anti-IL-6, anti-TNF- $\alpha$ , anti-p65 and anti-CD68) (1:200) were mixed with the tissue sections overnight at 4 °C. Then, the slices were incubated with secondary antibodies coupled to FITC or rhodamine at room temperature for 1 h. After rinsing, DAPI was used to stain the nuclei. Images for each tissue section were obtained by a confocal microscope (Nikon) at a magnification of 200. Use at least three coverslips for each experimental group [25].

2.15. Flow cytometry analysis of ROS

BV2 cells were incubated in the hypoxic condition and/or with different doses of YNFJ. Then samples were stained with 2 mM DHE at 37 °C for 30 min in a dark environment. ROS production was analyzed according to the ROS kit (Beyotime Biotechnology, Shanghai, China) using a flow cytometer (FACS Calibur™, BD Biosciences) [16].

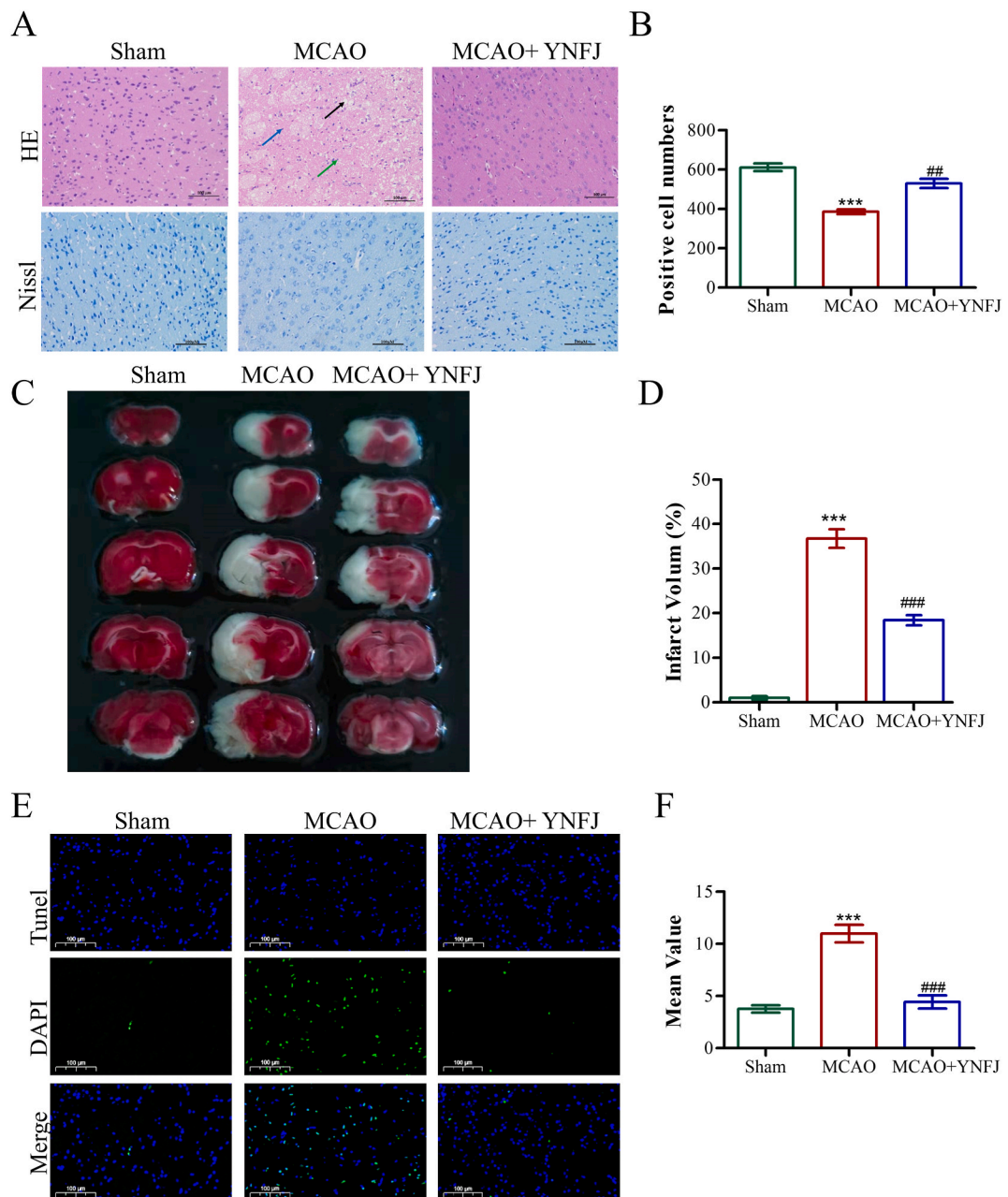


**Fig. 3.** YNFJ treatment relieved neuronal injury in the ischemic penumbra. (A) HE staining of rat brain tissue. Scale bars = 100 μm. The black arrow represented the irregular cavities. The blue arrow represented the pyknotic nuclei of neuron. The green arrow represented the macrophage infiltration in the ischemic penumbra. Nissl staining was shown under the HE staining. Scale bars = 100 μm. (B) The quantified number of nerve cells in Nissl staining. (C, D) TTC-stained brain sections and quantitative analysis of infarct volume in different groups. (E, F) TUNEL staining and the quantitative analysis. n = 5 rats (5 slices in each rat) in each group. Scale bars = 100 μm \*\*\*p < 0.001 vs. sham group; ##p < 0.01, ###p < 0.001 vs. MCAO model group. n = 5 per group.

## 2.16. Statistical analysis

For enrichment analysis in network pharmacology (GO&KEGG), a Hypergeometric distribution test followed by FDR correction was applied. It is considered to be compared with the whole genome background, take corrected-pvalue <0.05 as the threshold. For experimental verification section, data were expressed as mean  $\pm$  standard deviation (SD) and were deeply analyzed using SPSS 19 and GraphPad Prism 6.0 (GraphPad Software). When the result conforms to or approximately conforms to the Normal distribution, One-way analysis of variance (ANOVA) followed by Turkey's post hoc test were adopted for multiple comparisons. Differences at  $p < 0.05$  were considered significant. Each experiment was repeated for more than 3 times independently.

**Table 2**

Description of YNFJ active ingredients.

MolID	MolName	Herb(s)
MOL000006	luteolin	Carthami Flos
MOL000098	quercetin	Typhae Pollen, Carthami Flos, Notoginseng Radix Et Rhizoma
MOL0000X1	peoniflorin	Paeoniae Radix Rubra
MOL0000X2	rutoside	Sophorae Flos
MOL0000X3	Isorhamnetin-3-O-neohesperidoside	Typhae Pollen
MOL0000X4	notoginsenoside R1	Notoginseng Radix Et Rhizoma
MOL0000X5	ginsenoside Rg1	Notoginseng Radix Et Rhizoma
MOL0000X6	ginsenoside Rb1	Notoginseng Radix Et Rhizoma
MOL0000X7	glutamic acid	Pheretima
MOL0000X8	cholesterol	Pheretima
MOL000131	linolenic acid	Pheretima
MOL000296	hederagenin	Siegesbeckiae Herba
MOL000354	isorhamnetin	Typhae Pollen, Carthami Flos
MOL000358	beta-sitosterol	Paeoniae Radix Rubra, Typhae Pollen, Carthami Flos, Puerariae Lobatae Radix, Sophorae Flos, Siegesbeckiae Herba
MOL000359	sitosterol	Paeoniae Radix Rubra, Chuanxiong Rhizoma
MOL000392	formononetin	Puerariae Lobatae Radix
MOL000422	kaempferol	Typhae Pollen, Carthami Flos
MOL000433	FA	Chuanxiong Rhizoma, Pheretima
MOL000449	Stigmasterol	Paeoniae Radix Rubra, Carthami Flos, Siegesbeckiae Herba, Notoginseng Radix Et Rhizoma
MOL000492	catechin	Paeoniae Radix Rubra
MOL000675	oleic acid	Pheretima
MOL000953	CLR	Carthami Flos, Pheretima
MOL001002	ellagic acid	Paeoniae Radix Rubra
MOL001040	(2R)-5,7-dihydroxy-2-(4-hydroxyphenyl)chroman-4-one	Typhae Pollen
MOL0000X9	arachidonic acid	Typhae Pollen, Pheretima
MOL001494	Mandenol	Chuanxiong Rhizoma, Siegesbeckiae Herba
MOL001792	DFV	Notoginseng Radix Et Rhizoma
MOL001924	paeoniflorin	Paeoniae Radix Rubra
MOL002135	Myricanone	Chuanxiong Rhizoma
MOL002140	Perlolyrine	Chuanxiong Rhizoma
MOL002157	wallichilide	Chuanxiong Rhizoma
MOL002694	4-[(E)-4-(3,5-dimethoxy-4-oxo-1-cyclohexa-2,5-dienylidene)but-2-enylidene]-2,6-dimethoxycyclohexa-2,5-dien-1-one	Carthami Flos
MOL002695	lignan	Carthami Flos
MOL002710	Pyrethrin II	Carthami Flos
MOL002712	6-Hydroxykaempferol	Carthami Flos
MOL002714	baicalin	Paeoniae Radix Rubra, Carthami Flos, Siegesbeckiae Herba, Notoginseng Radix Et Rhizoma
MOL002717	qt_carthamone	Carthami Flos
MOL002721	quercetagenin	Carthami Flos
MOL002757	7,8-dimethyl-1H-pyrimido [5,6-g]quinoxaline-2,4-dione	Carthami Flos
MOL002773	beta-carotene	Carthami Flos
MOL002776	Baicalin	Carthami Flos
MOL002879	Diop	Notoginseng Radix Et Rhizoma
MOL002959	3'-Methoxydaidzein	Puerariae Lobatae Radix
MOL004177	15alpha-Hydroxy- <i>ent</i> -kaur-16-en-19-oic acid	Siegesbeckiae Herba
MOL004179	Vernolic acid	Siegesbeckiae Herba
MOL004180	Coronaridine	Siegesbeckiae Herba
MOL004184	Siegesesteric acid II	Siegesbeckiae Herba
MOL004185	Siegesmethyletheric acid	Siegesbeckiae Herba
MOL004355	Spinasterol	Paeoniae Radix Rubra
MOL005344	ginsenoside rh2	Notoginseng Radix Et Rhizoma
MOL005500	linolenate	Pheretima
MOL005935	N-[6-(9-acridinylamino)hexyl]benzamide	Sophorae Flos
MOL006992	(2R,3R)-4-methoxyl-distylin	Paeoniae Radix Rubra
MOL011418	lysolecithin	Pheretima

### 3. Results

#### 3.1. YNFJ treatment relieved neuronal injury in the ischemic penumbra of rat

In order to observe the relieving effect of YNFJ on the neuronal injury of MCAO rats, we used HE and Nissl staining to observe the ischemic penumbra. HE results showed that (Fig. 3A), the number of cortical neurons in the sham operation group was abundant, evenly and neatly distributed. However, rats in the MCAO group had a large area of cortex infarction, and a large number of eosinophils and irregular cavities (black arrows). As shown by the blue arrow in the figure, many neuron nuclei can be seen pyknotic and deeply stained, irregular in shape. Moreover, macrophage infiltration (Green arrow) was observed in the ischemic penumbra. YNFJ treatment significantly improved the cells to have a clear outline, intact nucleolus, and compact structure. After Nissl staining (Fig. 3A and B), the positive cells (Nissl +) in the sham group had intact neurons, while the neurons in the MCAO group had atrophied cell bodies and were accompanied by atrophied nuclei. The number of Nissl + cells in the Sham group was  $610.33 \pm 34.27$ , and  $384.67 \pm 20.26$  in the MCAO group. YNFJ treatment significantly promoted the number of Nissl + cells to  $528.33 \pm 40.22$ . TTC staining displayed that the infarct volume of rats in MCAO group reached 36.73 % in relative to that in the sham group. However, YNFJ application significantly decreased the infarct volume to 18.37 % (Fig. 3C, D). As the results of tunel staining showed in Fig. 3E and F, the mean value of the Sham group was  $3.76 \% \pm 0.63 \%$ . MCAO group significantly increased to  $10.98 \% \pm 1.47 \%$ , while the YNFJ treatment group decreased it to  $4.44 \% \pm 1.07 \%$ . These results indicated that the neuronal injury was alleviated by YNFJ treatment in the ischemic penumbra.

#### 3.2. YNFJ-target-IS (ischemic stroke) network construction and core target screening

Through the published literature, 279 potential targets for 54 active compounds (Table 2) were obtained. By GeneCards, DrugBank and OMIM databases, 2977 therapeutic targets for ischemic stroke were collected, and 189 common potential targets against ischemic stroke were obtained after comparing the targets of YNFJ and ischemic stroke (Fig. 4A). The network topology parameters of YNFJ and ischemic stroke were analyzed using Gephi 0.9.2 software to identify the relationship between the corresponding compounds, which contained 198 nodes and 687 edges (Fig. 4B).

#### 3.3. PPI network construction

The PPI network was constructed to further analyze the key targets of YNFJ in ischemic stroke treatment by using CytoNCA plugin for cytoscape 3.9.1, as shown in Fig. 5A, which consisted of 65 nodes and 1519 edges (Fig. 5A). According to the degree principle of each target, the top 30 core targets by string analysis were shown in Fig. 5B. Moreover, the key effective compounds of YNFJ and their corresponding target proteins were shown in Table 3. Combined the core protein analysis with literature comparison, we found that IL6 (IL-6), TNF (TNF- $\alpha$ ), PTGS2 (COX2), NFKBIA ( $\text{I}\kappa\text{B}\alpha$ ) and NFE2L2 (Nrf2) were most likely to be the key targets for revealing the mechanism of YNFJ treatment for ischemic stroke (Fig. 5C).

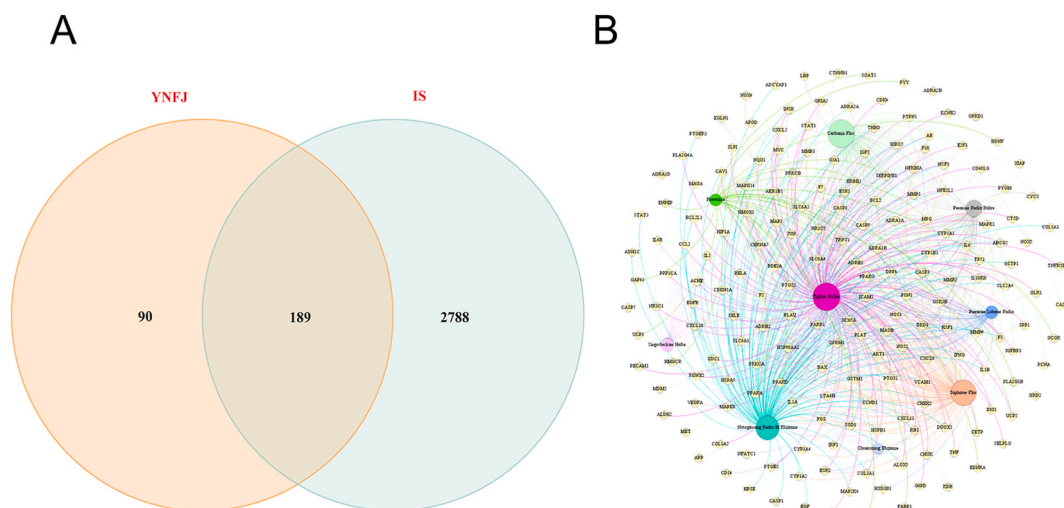


**Fig. 4.** The construction of YNFJ-target-IS. (A) Venn diagram describing targets distribution of YNFJ and IS. (B) YNFJ-target-IS network. The colored circles represent Latin names of drugs in YNFJ, and the yellow circles represent target proteins associated with IS.

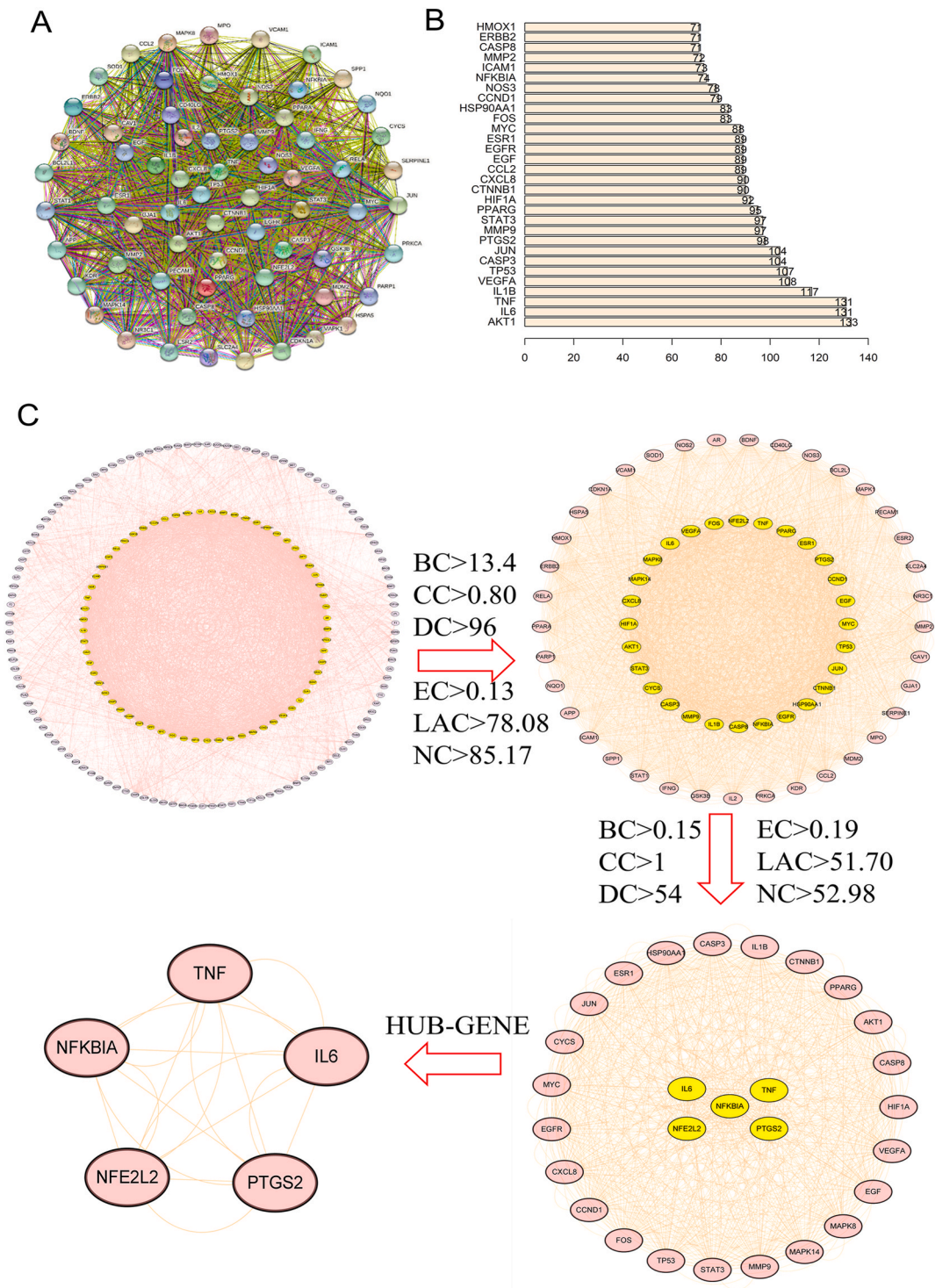


**Fig. 5.** Protein–protein interaction (PPI) network of YNFJ target for the treatment of IS. (A) Hub genes of YNFJ for IS. The top 65 key targets were screened using the Cytoscape plugin. PTGS2, NFKBIA and NFE2L2 stands for COX2, IKB $\alpha$  and Nrf2 as its gene name, respectively. (B) STRING analysis of YNFJ targets for treating IS. The statistical analysis was on the right, in which X-axis represented the number of network neighbor nodes, and Y-axis represented the name of the protein.

**Table 3**  
Key effective compounds of YNFJ and their corresponding target proteins.

MolId	MolName	Degree	Herb(s)	Symbols
MOL000098	Quercetin	515	Typhae Pollen Carthami Flos, Notoginseng Radix Et Rhizoma	AR,PPARG, PTGS2,HSP90AA1,NCOA2,DPP4,AKR1B1, PRSS1, TOP2A, F2, KCNH2, SCN5A, F10, ADRB2, MMP3, PRKACA, F7, RXRA, ACHE, MAOB, RELA, EGFR, AKT1, CCND1, BCL2, BCL2L1, FOS, CDKN1A, EIF6, BAX, CASP9, PLAU, MMP2, MMP9, MAPK1, IL10RB, RB1, TNFAIP6, JUN, IL6, AHS1, CASP3, TP53, ELK1, NFKBIA, ODC1, CASP8, TOP1, RAF1, SOD1, PRKCA, MMP1, HIF1A, STAT1, RUNX1T1, CDK1, HSPA5, ERBB2, PPARG, ACACA, HMOX1, CYP3A4, CAV1, MYC, F3, GJA1, CYP1A1, ICAM1, IL1B, CCL2, SELE, VCAM1, CXCL8, PRKCB, BIRC5, DUOX2, NOS3, HSPB1, IL2, NR1I2, CYP1B1, CCNB1, PLAT, THBD, SERPINE1, IFNG, ALOX5, IL1A, MPO, TOP2A, NCF1, ABCG2, HAS2, NFE2L2, NQO1, PARP1, AHR, PSMD3, SLC2A4, COL3A1, CXCL11, CXCL2, DCAF5, NR1I3, CHEK2, INSR, CLDN4, PPARA, PPARD, HSF1, CXCL10, CHUK, SPP1, RUNX2, RASSF1, E2F1, E2F2, ACP3, CTSD, IGF2, IGF2R, CD40LG, IRF1, ERBB3, PON1, DIO1, PCOLCE, NPEPPS, HK2, RASA1, GSTM1, GSTM2, PTGS1
MOL000358	Beta-sitosterol	261	Paeoniae Radix Rubra Typhae Pollen, Carthami Flos, Puerariae Lobatae Radix, Sophorae Flos, Siegesbeckiae Herba	PGR, NCOA2, PTGS1, PTGS2, HSP90AA1, KCNH2, PRKACA, DRD1, CHRM3, CHRM1, SCN5A, CHRM4, PDE3A, ADRA1A, CHRM2, ADRA1B, ADRB2, CHRNA2, SLC6A4, OPRM1, CHRNA7, BCL2, BAX, CASP9, JUN, CASP3, CASP8, PRKCA, PON1, MAP2
MOL000422	Kaempferol	110	Typhae Pollen Carthami Flos	NOS2, PTGS1, AR, PPARG, PTGS2, HSP90AA1, PRKACA, NCOA2, DPP4, PRSS1, PGR, F2, CHRM1, ACHE, SLC6A2, CHRM2, ADRA1B, TOP2A, F7, PCP4, RELA, IKKB, AKT1, BCL2, BAX, TNFAIP6, JUN, AHS1, CASP3, MAPK8, MMP1, STAT1, CDK1, PPARG, HMOX1, CYP3A4, CYP1A1, ICAM1, SELE, VCAM1, NR1I2, CYP1B1, ALOX5, HAS2, AHR, PSMD3, SLC2A4, NR1I3, INSR, DIO1, PPP3CA, GSTM1, GSTM2, AKR1C3, SLPI
MOL000449	Stigmasterol	108	Paeoniae Radix Rubra Carthami Flos, Siegesbeckiae Herba, Notoginseng Radix Et Rhizoma	PGR, NR3C2, NCOA2, IGHG1, RXRA, NCOA1, PTGS1, PTGS2, ADRA2A, SLC6A2, SLC6A3, ADRB2, AKR1B1, PLAU, LTA4H, MAOB, MAOA, PRKACA, CTRB1, CHRM3, CHRM1, ADRB1, SCN5A, ADRA1A, CHRM2, ADRA1B, CHRNA7
MOL002714	Baicalein	70	Paeoniae Radix Rubra Carthami Flos, Siegesbeckiae Herba, Notoginseng Radix Et Rhizoma	PTGS1, AR, PTGS2, HSP90AA1, PRKACA, DPP4, PDE3A, PRSS1, NCOA2, NCOA1, PCP4, RELA, AKT1, BCL2, FOS, BAX, MMP9, CASP3, TP53, HIF1A, FOSL1, FOSL2, CDK1, CCNB1, MPO, AHR, IGF2, CYCS, NFATC1, TDRD7, EGLN1, NOX5, FABP5, APOD, F10, PTPN1
MOL000354	Isorhamnetin	60	Typhae Pollen Carthami Flos	NOS2, PTGS1, ESR1, AR, PPARG, PTGS2, PTPN1, ESR2, DPP4, MAPK14, GSK3B, HSP90AA1, CDK2, PRKACA, PRSS1, CCNA2, NCOA2, PCP4, PYGM, PPARD, CHEK1, AKR1B1, NCOA1, F7, F2, ACHE, MAOB, GRIA2, RELA, NCF1, OLR1
MOL000006	luteolin	53	Carthami Flos	PTGS1, AR, PTGS2, HSP90AA1, PRSS1, NCOA2, PRKACA, DPP4, RELA, EGFR, AKT1, CCND1, BCL2L1, CDKN1A, CASP9, MMP2, MMP9, MAPK1, IL10RB, RB1, CDK4, TNFAIP6, JUN, IL6, CASP3, TP53, NFKBIA, TOP1, MDM2, APP, MMP1, PCNA, ERBB2, PPARG, HMOX1, CASP7, ICAM1, MCL1, BIRC5, IL2, CCNB1, TYR, IFNG, IL4R, TOP2A, XIAP, SLC2A4, INSR, CD40LG, PTGES, NUF2, ADCY2, MET
MOL000675	Oleic acid	39	Pheretima	PTGS1, NCOA2, PTGS2, LYZL4, PRSS3, RXRA, PLAU, SOD1, TEPI, EDNRA, ERBB2, PPARG, LPL, GAP43, SERPINE1, BDNF, HMGCGR, MPO, PPARA, PPARD, PON1, TMEM219, PLGLA, FABP1, RBP2, GCGR, ENPEP, UCP2, SOAT1, CCKAR, CITED1, PDX1, SLC2A2, PAM, SCD, UCP3, CETP, PYY, DNPEP, PTGS1, PTGS2, RXRA, TRPV1, RXRG, SLC6A2, RELA, CCND1, MAPK1, CDK4, CASP3, PPARG, G6PD, PRKCB, PECAM1, NOS3, ALOX5, PLA2G4A, SELPLG, PTGES, GLB1, ALDH2, ABCA1, UCP2, C1R, CETP, ABCC4, KCNK10, TNFRSF1B, PTGES2, KCNK2, COL1A2
MOL0000X9	Arachidonic acid	36	Typhae Pollen Pheretima	NOS2, PTGS1, CHRM1, ESR1, AR, PPARG, PTGS2, RXRA, PDE3A, ADRA1A, SLC6A3, ADRB2, SLC6A4, ESR2, DPP4, MAPK14, GSK3B, HSP90AA1, CDK2, MAOB, CHEK1, PRKACA, PRSS1, CCNA2, PCP4, PKIA, F2, ACHE, DPEP1, JUN, PPARG, IL4R, ATP5F1B, HSD3B2, HSD3B1
MOL000392	Formononetin	35	Puerariae Lobatae Radix	

### 3.4. GO and KEGG enrichment analyses

We subjected the obtained 189 intersecting genes to GO and KEGG analysis to acquire enriched functional clusters. GO enrichment analysis showed that 7461 GO items were obtained, among which CC, MF and BP were 262, 910 and 6289, respectively. In addition, the items with  $p < 0.05$  in these three sections were 286, 465 and 3987, respectively. Furthermore, the bubble chart of CC showed that targets of YNFJ occurred primarily at membrane raft, membrane microdomain, and membrane region (Fig. 6A). Clearly, MF was

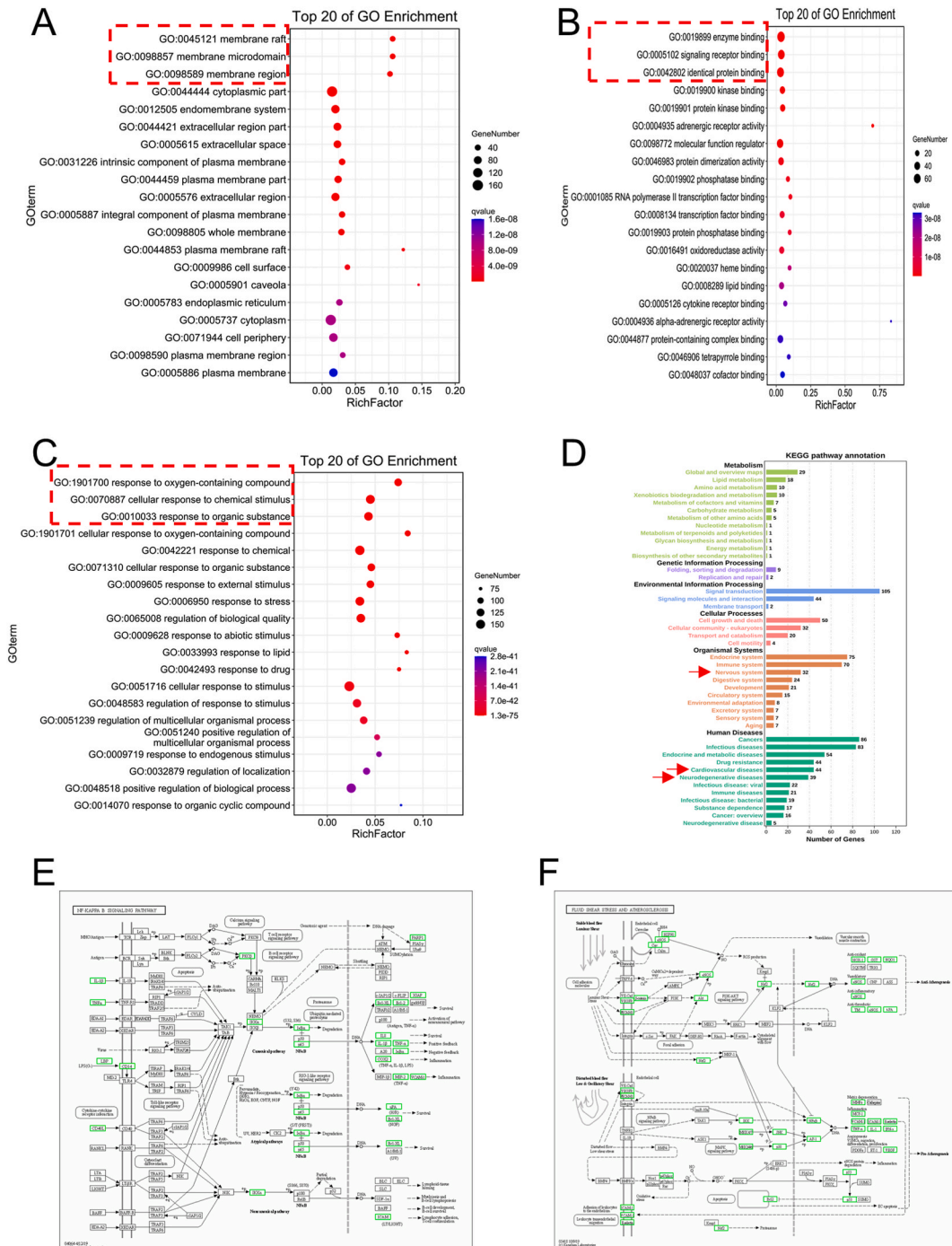


**Fig. 6.** GO and KEGG Enrichment Analyses. Top 20 of GO enrichment analysis for target genes based on the cellular component (A), molecular function (B), biological process (C). (D) KEGG annotation analysis for the top 20 targets. (E) NF-κB signaling pathway (has: 04064) related to YNFJ for IS. (F) Fluid shear stress and atherosclerosis signaling pathway (has:05418) related to YNFJ for IS.

mainly associated with the enzyme binding, signaling receptor binding and identical protein binding (Fig. 6B). The results of BP indicated that targets of YNFJ for treatment on ischemic stroke were closely related to the positive regulation of response to oxygen-containing compounds, cellular response to chemical stimulus and response to organic substance (Fig. 6C). For KEGG enrichment analysis, we obtained 162 KEGG items. We used OmicShare platform and R language software to reveal the pathway diagram of YNFJ in the treatment of ischemic stroke. As shown in Fig. 6D, nervous system, cardiovascular diseases and neurodegenerative diseases were highly enriched pathways. As shown in Table 4, we found that there are three pathways related to inflammation in the top 20 pathways. Combining the results of hubgene (IL6, TNF, PTGS2, NFKBIA and NFE2L2) and pathway enrichment, the NF $\kappa$ B signaling pathway (has: 04064) and fluid shear stress and atherosclerosis signaling pathway (has:05418) were closely associated with the treatment of ischemic stroke with YNFJ (Fig. 6E and F).

### 3.5. YNFJ treatment inhibited the release of inflammatory factors on microglia in the ischemic penumbra

The previous results showed that, IL-6 and TNF were two key proteins obtained in the PPI analysis, indicating that the mechanism of YNFJ is closely related to the inhibition of neuroinflammation. Inflammation is a pivotal process in the pathogenesis of acute ischemic stroke [26]. To study the inhibitory effect of YNFJ on inflammation, ELISA was firstly adopted to detect the secreted levels of IL-6 and TNF- $\alpha$ . We observed that IL-6 in the MCAO group increased from 14.36 pg/mL (in sham group) to 113.16 pg/mL, while YNFJ reduced it to 52.10 pg/mL (Fig. 7A). Consistently, the level of TNF- $\alpha$  in the MCAO group increased from 4.62 pg/mL (in sham group) to 21.50 pg/mL, and YNFJ decreased it to 9.82 pg/mL (Fig. 7B).

Microglia is a type of glial cells, equivalent to macrophages in the brain, which is the first and most important line of immune defense in the CNS [27]. In this study, we used CD38, a microglia marker, to mark microglia (red), and used immunofluorescence to detect the expression of IL-6 (green) and TNF- $\alpha$  (green) in microglia. As shown in Fig. 7C, MCAO administration significantly up-regulated the levels of IL-6 and TNF- $\alpha$ , which were decreased by YNFJ effectively. Thus, YNFJ treatment inhibited the release of

**Table 4**  
The top 20 KEGG pathways.

Pathway ID	KEGG_A_class	KEGG_B_class	Pathway	Pvalue	FDR
ko04933	Human Diseases	Endocrine and metabolic diseases	AGE-RAGE signaling pathway in diabetic complications	2.55E-33	6.76E-31
ko05200	Human Diseases	Cancers	Pathways in cancer	7.37E-31	9.77E-29
ko05418	Human Diseases	Cardiovascular diseases	Fluid shear stress and atherosclerosis	7.10E-28	6.27E-26
ko05167	Human Diseases	Infectious diseases	Kaposi sarcoma-associated herpesvirus infection	5.86E-23	3.88E-21
ko05161	Human Diseases	Infectious diseases	Hepatitis B	7.30E-22	3.87E-20
ko05163	Human Diseases	Infectious diseases	Human cytomegalovirus infection	3.74E-21	1.56E-19
ko04668	Environmental Information Processing	Signal transduction	TNF signaling pathway	4.13E-21	1.56E-19
ko05215	Human Diseases	Cancers	Prostate cancer	6.93E-20	2.29E-18
ko04657	Organismal Systems	Immune system	IL-17 signaling pathway	2.45E-19	7.22E-18
ko05219	Human Diseases	Cancers	Bladder cancer	4.14E-18	1.10E-16
ko05160	Human Diseases	Infectious diseases	Hepatitis C	7.65E-17	1.84E-15
ko05212	Human Diseases	Cancers	Pancreatic cancer	2.97E-16	6.55E-15
ko05205	Human Diseases	Cancers	Proteoglycans in cancer	1.01E-15	2.05E-14
ko05145	Human Diseases	Infectious diseases	Toxoplasmosis	2.01E-15	3.80E-14
ko01522	Human Diseases	Drug resistance	Endocrine resistance	4.17E-15	7.37E-14
ko05222	Human Diseases	Cancers	Small cell lung cancer	6.69E-15	1.11E-13
ko04620	Organismal Systems	Immune system	Toll-like receptor signaling pathway	9.32E-15	1.45E-13
ko05162	Human Diseases	Infectious diseases	Measles	1.03E-14	1.51E-13
ko05210	Human Diseases	Cancers	Colorectal cancer	8.92E-14	1.24E-12
ko04066	Environmental Information Processing	Signal transduction	HIF-1 signaling pathway	1.01E-13	1.01E-13

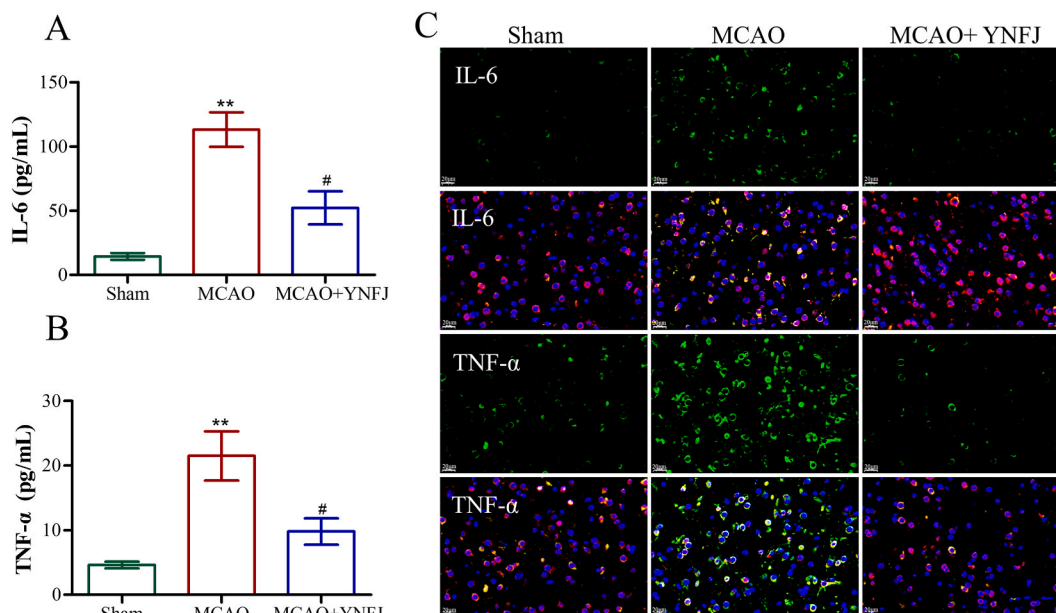


**Fig. 7.** YNFJ treatment inhibited the release of inflammatory factors on microglia in the ischemic penumbra. (A, B) The protein expression of IL-6 and TNF- $\alpha$  were measured by ELISA. (C) Images of co-localized immunofluorescence reactivity of IL-6 (green, FITC; blue, DAPI) and TNF- $\alpha$  (green, FITC; blue, DAPI) in the regions of ischemic penumbra. CD68 (red) is a marker for microglial cells. N = 5 per group. Scale bar = 20  $\mu$ m \*\*p < 0.01, vs. sham group; #p < 0.05 vs. MCAO model group. n = 3 per group.

inflammatory factors from microglia in the ischemic penumbra.

### 3.6. YNFJ treatment inhibited p65 NF- $\kappa$ B activation on microglia in the ischemic penumbra

KEGG enrichment analysis showed that NF- $\kappa$ B was a key pathway for YNFJ on ischemic stroke. Therefore, we further analyzed the effect of YNFJ on NF- $\kappa$ B activation by measuring the associated protein expressions. In the current study, we observed that MCAO group had promoted the expression of p-I $\kappa$ B $\alpha$  (~2.94 fold) and p-p65/p65 (~3.80 fold) in comparison to controls (Sham), whereas YNFJ treatment can significantly reduce their levels, compared to the MCAO group (Fig. 8A). The results of immunofluorescence also showed that nuclear translocation of p65 was enhanced in microglia (CD68<sup>+</sup>, Fig. 8C), but not in neurons (MAP2+, Fig. 8D), in MCAO rats. And YNFJ treatment inhibited the nuclear metastasis of p65. Moreover, we observed a significant increase in iNOS and COX2 expression in the ischemic penumbra, which were also decreased by YNFJ (Fig. 8B). These results indicated that YNFJ inhibited inflammation by inhibiting NF- $\kappa$ B activation in the ischemic penumbra.

### 3.7. YNFJ treatment inhibited oxidative stress in the ischemic penumbra

Our study found that YNFJ had a strong anti-oxidant effect in MCAO rats. Results indicated that the activity of SOD was reduced in MCAO group than that in Sham group. And YNFJ treatment increased SOD levels significantly (Fig. 9A). MDA was found to be significantly promoted in the ischemic penumbra contrasted to that in sham, but was markedly prevented by YNFJ treatment compared with MCAO group (Fig. 9B).

Loboda's team demonstrated that Nrf2 and HO-1, are key factors in regulating the molecular mechanism in alleviating oxidative stress under neuron damage conditions [28]. Our network pharmacology results also enriched that the Nrf2/HO-1 pathway contained in the fluid shear stress and atherosclerosis signaling pathway is the major role in the treatment of ischemic stroke by YNFJ. Our findings showed that after treated with YNFJ, nuclear translocation of Nrf2 was enhanced, accompanied with the decreased level of cytoplasmic expression of Nrf2 in relative to MCAO group (Fig. 9C). Moreover, YNFJ reduced the expression of Keap-1 (Fig. 9C). Consistently, YNFJ markedly enhanced the levels of HO-1 and NQO-1 (Fig. 9D). These results indicated that YNFJ treatment inhibited oxidative stress via Nrf2/HO-1 pathway.

### 3.8. YNFJ treatment decreased inflammation by inhibiting p65 NF- $\kappa$ B activation in hypoxia-induced BV2 cells

*In vitro* cell model was constructed for the further analysis of the possible influences of YNFJ on ischemic stroke. We then investigated the anti-inflammation properties of YNFJ to inhibit NF- $\kappa$ B activation in hypoxia-induced BV2 cells. ELISA analysis of YNFJ showed that IL-6 and TNF- $\alpha$  in BV2 cells treated with YNFJ were both significantly reduced in relative to the model group (Fig. 10A and B). In addition, the protein levels of key proteins in p65 NF- $\kappa$ B activation in BV2 cells were further studied. The findings revealed a

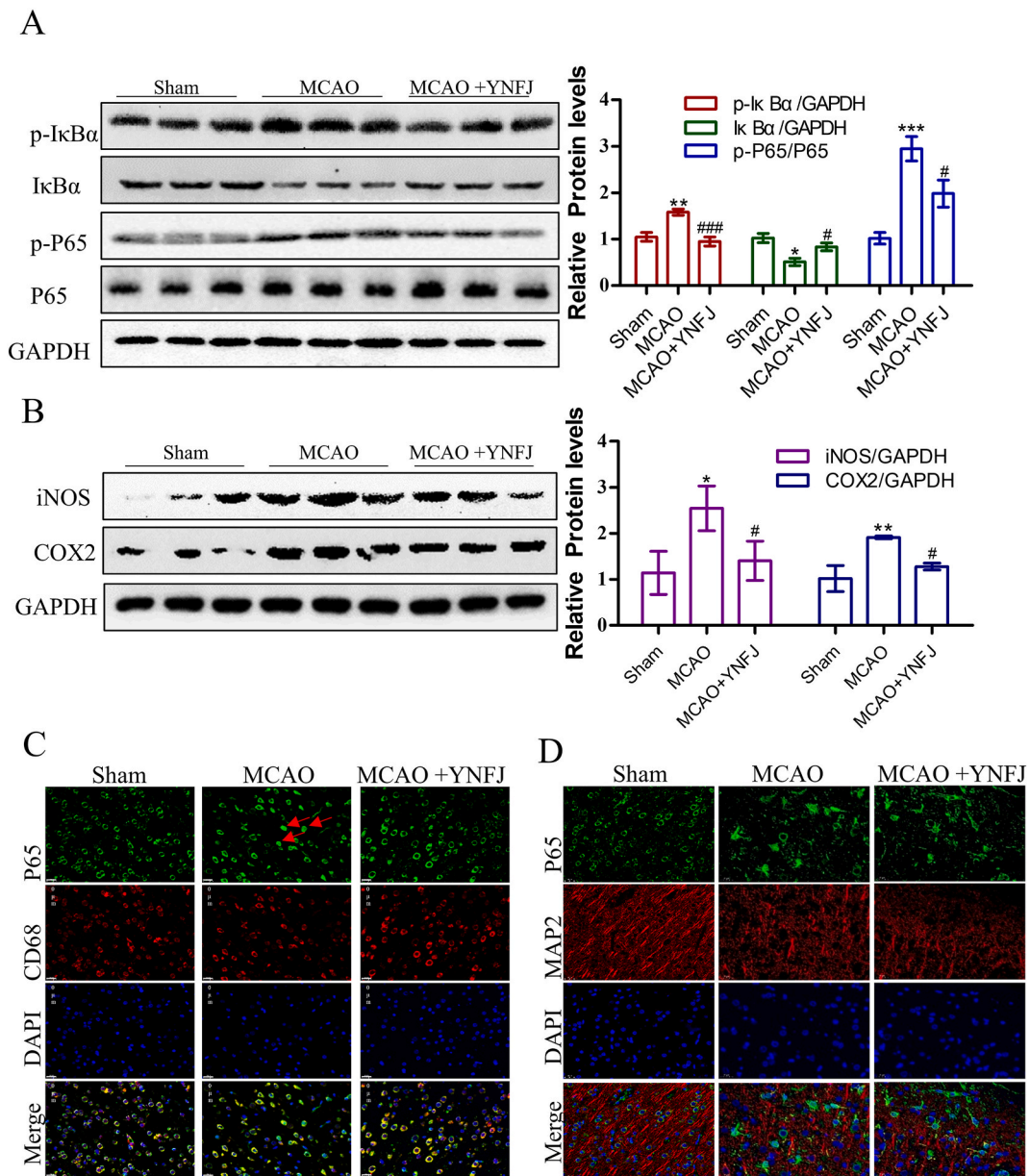


**Fig. 8.** YNFJ treatment inhibited p65 NF-κB activation on microglia in the ischemic penumbra. (A, B) Western blot analysis of the protein level of p-IκBα (Sup F.1), IκBα (Sup F.2), p-p65 (Sup F.3), p65 (Sup F.4), iNOS (Sup F.6) and COX2 (Sup F.7) in the ischemic penumbra. GAPDH (Sup F.5, 8) was an internal control. (C) The expression of p65 (green, FITC; red, CD68; blue, DAPI) was detected by immunofluorescence. (D) The expression of p65 (green, FITC; red, MAP2; blue, DAPI) was detected by immunofluorescence. Scale bars = 20 μm \*p < 0.05, \*\*p < 0.01, \*\*\*p < 0.001 vs. sham group; #p < 0.05, ###p < 0.001 vs. MCAO model group. n = 6 per group.

marked promoted expression of p-IκBα and p-p65, implying the activation of NF-κB was triggered in hypoxia-induced BV2 cells (Fig. 10C). We obtained a significantly increased level of p-IκBα and p-p65 in model group, which was significantly inhibited by YNFJ treatment. Meanwhile, the expression level of IκBα was down-regulated which was reserved by the YNFJ treatment. Consistently, the expression of iNOS and COX2 were reduced in the hypoxia-induced BV2 cells after receiving the YNFJ treatment (Fig. 10D). Therefore, the anti-inflammation effects of YNFJ could be attributed to inhibiting p65 NF-κB activation in hypoxia-induced BV2 cells.

### 3.9. YNFJ treatment inhibited oxidative stress by regulating Nrf2/HO-1 pathway in hypoxia-induced BV2 cells

BV2 cells were treated with/without YNFJ for 24 h and then incubated under hypoxic conditions (1%O<sub>2</sub>) for 12 h. Results showed that (Fig. 11A), the production of ROS in hypoxia-induced BV2 cells increased obviously compared to the control group, whereas

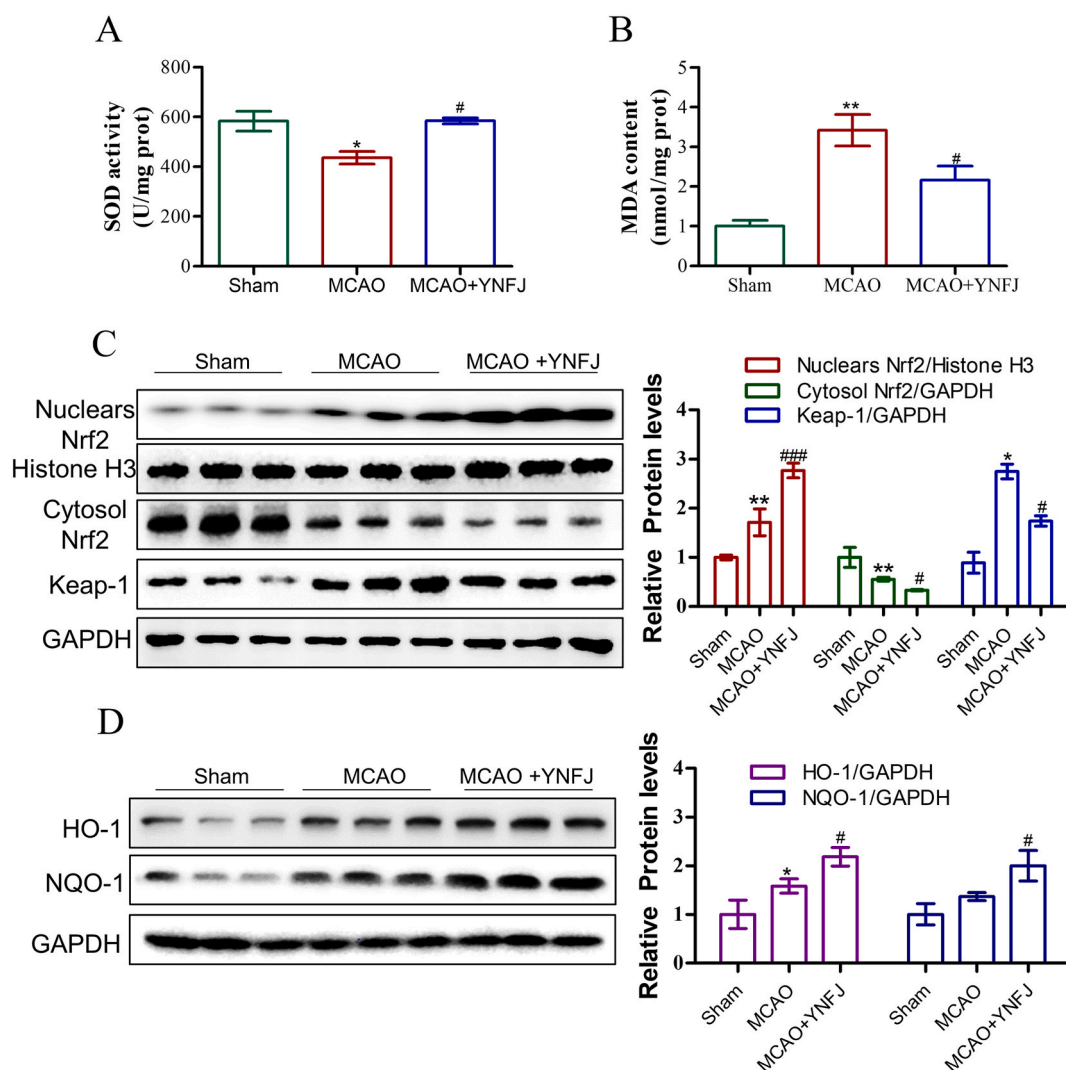


**Fig. 9.** YNFJ treatment inhibited oxidative stress in the ischemic penumbra. (A) A histogram of SOD activity in ischemic penumbra of MCAO rats. (B) A representative histogram of MDA content in ischemic penumbra of MCAO rats. (C, D) Western blot analysis of the protein level of Nuclears Nrf2 (Sup F.9), Cytosol Nrf2 (Sup F.11), Keap-1 (Sup F.12), HO-1 (Sup F.14) and NQO-1 (Sup F.15) in the ischemic penumbra. Histone H3 (Sup F.10) was the internal control of Nuclears Nrf2, and other proteins were GAPDH (Sup F.13, 16). \* $p < 0.05$ , \*\* $p < 0.01$  vs. sham group; # $p < 0.05$ , ### $p < 0.001$  vs. MCAO model group.  $n = 6$  per group.

different concentrations (50  $\mu\text{g/mL}$ , 100  $\mu\text{g/mL}$ , 200  $\mu\text{g/mL}$ ) of YNFJ treatment caused a significant decrease in their levels. Moreover, different concentrations of YNFJ enhanced the activity of SOD, but retained the content of MDA in a dose-dependent fashion, respectively (Fig. 11B and C). Results of Western blot showed that the ability of nuclear translocation of Nrf2 was enhanced by YNFJ treatment while the cytoplasmic expression of Nrf2 was suppressed by YNFJ application in hypoxia-induced BV2 cells. In addition, different concentrations of YNFJ cut back the expression of Keap-1, and dramatically accelerated the expression of HO-1 and NQO-1 (Fig. 11D–G). These results indicated that, consistent with *in vivo* experiments, YNFJ treatment restrained oxidative stress via Nrf2/HO-1 pathway in microglia.

#### 4. Discussion

YNFJ is an effective prescription for the clinical treatment of ischemic stroke, but its mechanism of action is unclear. Network pharmacology has become a new tactics for exploring the mechanism of medical treatment for diseases [29]. In this study, the mechanism of YNFJ treatment for ischemic stroke was found to be closely associated with NF $\kappa$ B signaling-mediated neuro-inflammation and Nrf2-mediated oxidative stress using network pharmacology analysis. However, these results were only found on database analysis and have not been experimentally verified. Thence, we validated the predicted results of network pharmacology by *in vitro* and *in vivo* experiments. The experimental results confirmed that, YNFJ improves ischemic stroke by inhibiting NF- $\kappa$ B and

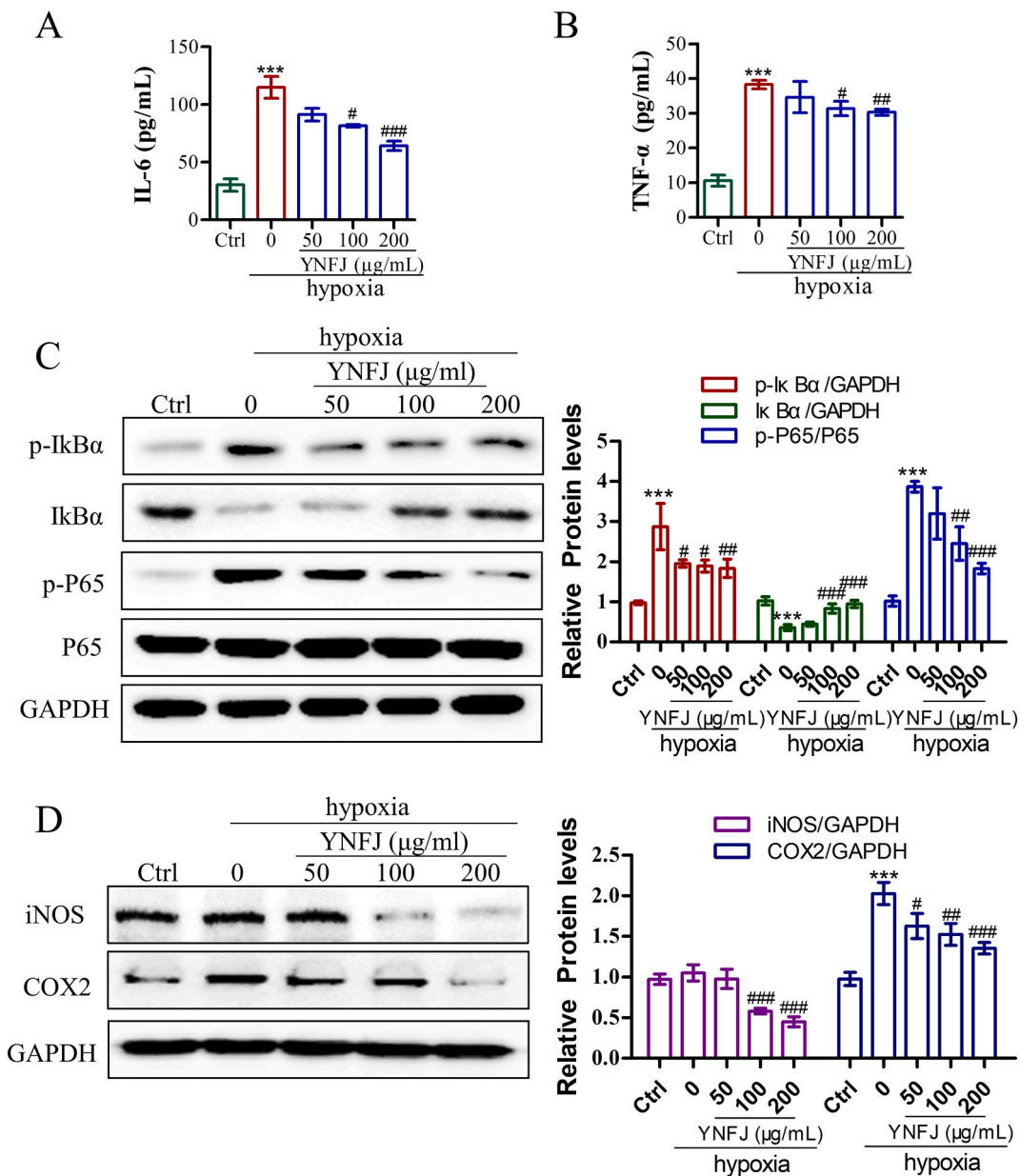


**Fig. 10.** YNFJ treatment decreased inflammation by inhibiting p65 NF-κB activation in hypoxia-induced BV2 cells. BV2 cells were treated with 1% O<sub>2</sub> for 12 h and/or YNFJ for 24 h. (A, B) The expression of IL-6 and TNF-α were measured by ELISA. (C, D) Western blot analysis of the protein level of p-IκBα (Sup F.17), IκBα (Sup F.18), p-p65 (Sup F.19), p65 (Sup F.20), iNOS (Sup F.22) and COX2 (Sup F.23) in BV2 cells. GAPDH (Sup F.21, 24) was an internal control. \*\*\*p < 0.001 vs. sham group; #p < 0.05, ##p < 0.01, ###p < 0.001 vs. hypoxia-induced model group. n = 3 per group.

activating Nrf2/HO-1 signaling pathways of microglia.

Our PPI combined with Hubgene analysis found that, 3 inflammation-related genes in the top 5 hub genes of YNFJ for ischemic stroke were screened, namely IL6 (IL-6), TNF (TNF-α), PTGS2 (COX2) (Fig. 5A). Moreover, KEGG enrichment analysis showed that (Table 4), there are 3 pathways related to inflammation in the top 20 pathways. Among the signaling pathways derived from KEGG enrichment analysis, many proteins in NFκB signaling pathway (has: 04064) were altered, and NF-κB signaling pathways participated in the process of cell survival and inflammation in ischemic stroke (Fig. 6D–F). Therefore, the mechanism of YNFJ on ischemic stroke was inseparable from inflammation. Inflammation is a crucial aspect of the pathological process of ischemic stroke [30]. The release of inflammatory factors (IL-6 and TNF-α) suddenly increases at least 48 h after MCAO [31,32]. In addition to these elevated pro-inflammatory cytokines, pro-inflammatory chemokines such as COX2, iNOS and NF-κB are also involved in the inflammatory pathology of MCAO injury [33]. In some studies, inhibition of NF-κB leads to neuroprotection [34,35]. Our results are consistent with the reported results, as MCAO increases the content of IL-6 and TNF-α, and the activation of NF-κB. However, YNFJ exerts an inhibitory

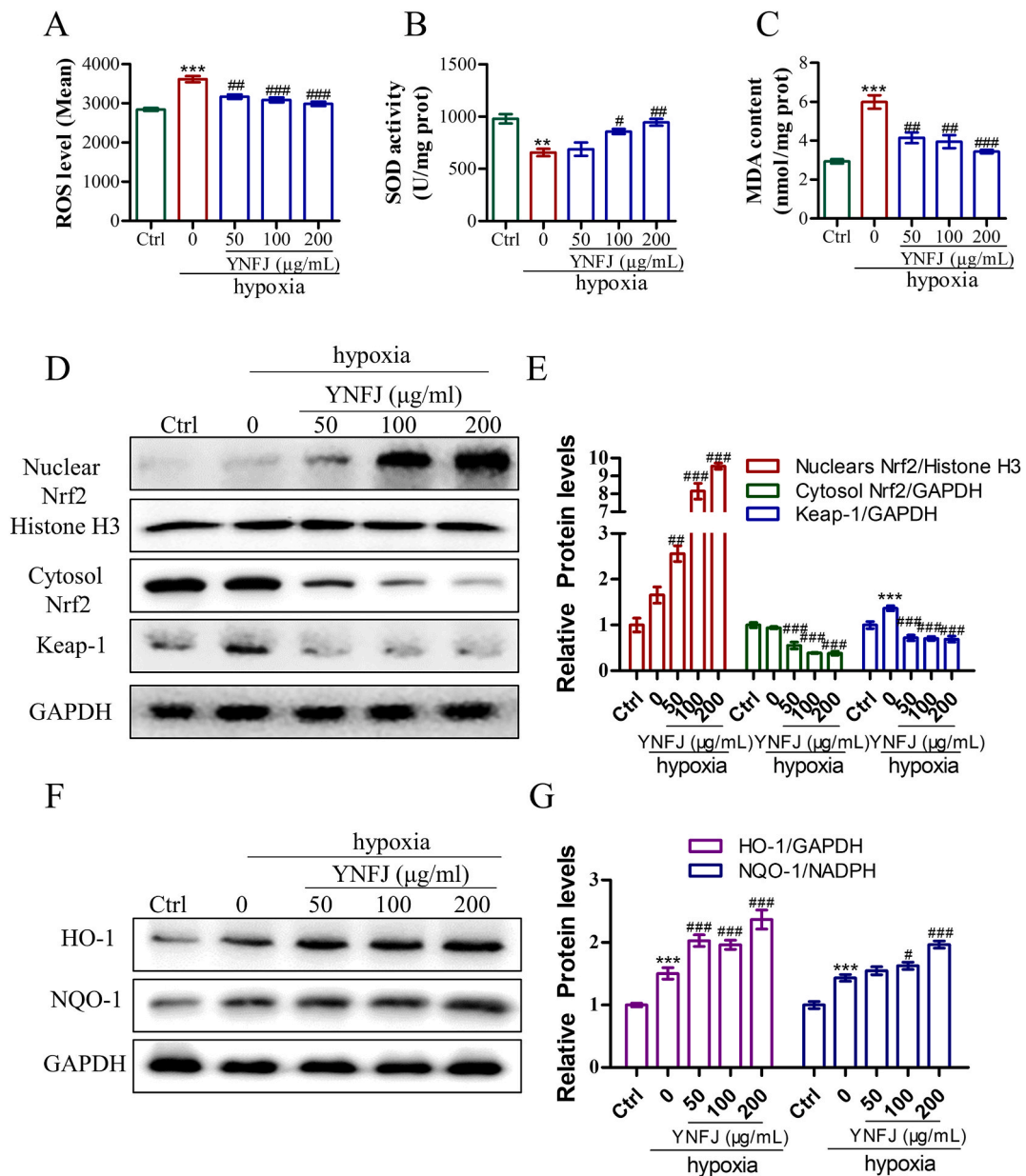


**Fig. 11.** YNFJ treatment inhibited oxidative stress by regulating Nrf2/HO-1 pathway in hypoxia-induced BV2 cells. BV2 cells were treated with/without YNFJ for 24 h and then incubated in 1%O<sub>2</sub> for 12 h. (A) The production of intracellular ROS is labeled with DCFH-DA fluorescent probe and detected by flow cytometry. (B, C) Representative histograms of SOD activity and MDA content in hypoxia-induced BV2 cells. (D–G) The protein levels of Nuclear Nrf2 (Sup F.25), Cytosol Nrf2 (Sup F.27), Keap-1 (Sup F.28), HO-1 (Sup F.30) and NQO-1 (Sup F.31) in BV2 cells. Histone H3 (Sup F.7) was the internal control of Nuclear Nrf2, and other proteins were GAPDH (Sup F.29, 32). \*\*\*p < 0.001 vs. sham group; #p < 0.05, ##p < 0.01, ###p < 0.001 vs. hypoxia-induced model group. n = 3 per group.

effect on NF-κB activation, and also reduces the expression of p-IκBα and the expression of chemokines, such as iNOS and COX2 (Fig. 8B). Similar to other reports, MCAO induced local brain tissue inflammatory response. We present here that, YNFJ can inhibit inflammatory damage by regulating NF-κB signaling pathways. In addition, many active ingredients in YNFJ have the same regulatory effect, such as *Panax notoginseng Saponins* [12], Ginsenoside Rb1 [36], Hydroxysafflor Yellow A [37], which provides support for the conclusions of this study. It is worth noting that we used CD68 to label microglia and MAP2 to label neurons, respectively. We found that YNFJ can inhibit the nuclear translocation of NF-κB in microglia (Fig. 8C). This effect is not obviously observed in neurons (Fig. 8D). Microglia are widespread throughout the CNS, and work as macrophages in the cellular immune process [38]. Interestingly, our study demonstrated that YNFJ may specifically target microglia in inhibiting inflammation. To further validate our findings, we established a hypoxia-induced microglia model to simulate ischemic stroke *in vitro*. Results strongly suggested that YNFJ reduced the

expression of IL6 and TNF- $\alpha$  by restraining the degradation of I $\kappa$ b- $\alpha$  and lessening the expression of p-P65 in hypoxia-induced BV2 cells (Fig. 10A–C).

A strong relationship between oxidative stress (OS) and inflammation is revealed in both neuronal and non-neuronal models [4]. Excess ROS accumulation in experimental ischemic stroke has long been established and well-studied [39]. Thus, OS is a rational method for investigating natural drug substances' antioxidative potential [40]. Our results of KEGG enrichment analysis showed that several proteins, such as Nrf2, HOX-1 (HO-1), NQO1, in the Nrf2/HO-1 signaling pathway were altered. And NFE2L2 (Nrf2) was one of the top 5 Hubgenes. As shown in Table 4, the fluid shear stress and atherosclerosis signaling pathway (has: 05418) with Nrf2/HO-1 as the key regulatory molecule ranks third in top 20. (However, the top two pathways were more closely related to diabetic applications and cancer, respectively.) Moreover, the role of Nrf2 in ischemic stroke and its potential neuroprotection have also been demonstrated using different ischemic stroke rodent models [41,42]. Therefore, we speculated that YNFJ exerted neuroprotective effects via Nrf2/HO-1 signaling pathway. Previous evidence pointed out that deficiency of Nrf2 leads to a great increase in infarct volume after 3 days of MCAO, which suggests that Nrf2 may play a valuable role in the pathological process of ischemic injury [43]. In our research, in comparison with Sham group, lower SOD levels and higher MDA levels were found in the MCAO group (Fig. 9A and B). After treated with YNFJ, the level of SOD was significantly increased and MDA level was reduced, which indicated that YNFJ reduced lipid peroxidation and restored the cellular anti-oxidant system by increasing SOD activity (Fig. 9A and B). Our previous research found that YNFJ can inhibit the accumulation of ROS, promote SOD and CAT activities, increase GSH-Px content, and reduce MDA content [5]. At present, we have obtained similar conclusions at animal level. In addition, we assessed that this antioxidant activity of YNFJ may be attributed to the activation of Nrf2 and its downstream HO-1 target, and then regulate and mobilize other endogenous antioxidant systems (Fig. 9C and D). In addition, many pharmacological components in YNFJ, such as Paeoniflorin [44], Puerarin [45], Hydroxysafflor Yellow A [46], have the effect of regulating the Nrf2/HO-1 pathway. Our present results are consistent with previous *in vitro* studies [5], and this observation supported the key role of brain strengthening in regulating Nrf2 in neuroinflammation. Accumulating evidence has revealed that, Nrf2 target genes are preferentially activated in glial cells compared to neurons and exert more pronounced anti-oxidant effects [47]. Therefore, in order to determine whether YNFJ specifically regulated microglia OS, we established a hypoxia-induced BV2 microglia cells model. *In vivo* experiments strongly suggested to us that YNFJ increased SOD activity and decreased MDA level by regulating Nrf2/HO-1 pathway, which is accordance with the *in vitro* findings (Fig. 11).

Our study first applied network pharmacology to identify potential targets and pathways for YNFJ treatment of IS. Then we validated the results of network pharmacology using MCAO animal models and hypoxia-induced BV2 cell models, combined with multiple biological methods to compensate for the limitations of network pharmacology methods and obtain more accurate and comprehensive results. Moreover, as shown in Table 5, we summarized the components and herbs involved in regulating the 5 Hubgenes in the experiment. The results indicate that some herbs, such as Chuanxiong Rhizoma, Puraria Lobatae Radix, Pheretima, and Siegesbeckiae Herba, have a targeted regulatory effect on PTGS2. And other herbs, such as Paeoniae Radix Rubra and Typhae Pollen, can simultaneously regulate multiple hubgenes. This reflects the characteristics of multi target and holistic views of traditional Chinese medicine. At the same time, it also provided some clues for our clinical flexible application. For example, we can make targeted adjustments to the herb and dosage of YNFJ based on the pathological characteristics and changes in key proteins of different stages of IS, in order to improve the individualized treatment effect of YNFJ. However, our research also has some limitations. The MCAO model is one of the commonly used animal models for studying human ischemic stroke. This model can simulate cerebral vascular occlusion and cerebral ischemia in ischemic stroke. Due to its strong controllability and simple operation, it has been widely used by researchers to explore the pathophysiological characteristics and mechanisms of ischemic stroke. However, there are species differences in anatomical structure, physiological process and drug metabolism between rats and humans. And there are also differences in the type, intensity, and timeline of immune responses. Therefore, although the MCAO model has the advantage of

**Table 5**  
The components and herbs involved in regulating the 5 Hubgenes.

Herb	Component(s)	Symbol(s)
Paeoniae Radix Rubra	ellagic acid , paeoniflorin , baicalein , beta-sitosterol , Stigmasterol , catechin , (2R,3R)-4-methoxyl-distylin	NFKBIA , IL6 , PTGS2
Chuanxiong Rhizoma	Mandenol , Myricanone , Perlolaryne , wallichilide	PTGS2
Typhae Pollen	(2R)-5,7-dihydroxy-2-(4-hydroxyphenyl)chroman-4-one , arachidonic acid , isorhamnetin , beta-sitosterol , kaempferol , quercetin,Isorhamnetin-3-O-neohesperidoside	PTGS2,IL6, NFKBIA, NFE2L2,TNF
Puerariae Lobatae Radix	formononetin,beta-sitosterol,3'-Methoxydaidzein	PTGS2
Carthami Flos	4-[(E)-4-(3,5-dimethoxy-4-oxo-1-cyclohexa-2,5-dienylidene)but-2-enylidene]-2,6-dimethoxycyclohexa-2,5-dien-1-one,lignan, Pyrethrin II,6-Hydroxykaempferol,baicalein, qt.carthamone,quercetagenin,7,8-dimethyl-1H-pyrimido [5,6-g]quinoxaline-2,4-dione,beta-carotene,beta-sitosterol,kaempferol, Stigmasterol,luteolin, quercetin	PTGS2,IL6, NFKBIA, NFE2L2
Sophorae Flos	isorhamnetin,beta-sitosterol,quercetin, rutoside,	PTGS2,IL6, NFKBIA, NFE2L2,TNF
Pheretima	arachidonic acid, linolenic acid, oleic acid, linolenate	PTGS2
Siegesbeckiae Herba	Vernolic acid, hederagenin,beta-sitosterol,Stigmasterol	PTGS2
Notoginseng Radix Et Rhizoma	Mandenol,DFV,beta-sitosterol,Stigmasterol, ginsenoside Rh2,quercetin	PTGS2,NFKBIA, IL6 ,NFE2L2

simulating human ischemic stroke, there are still some limitations. In our study, an additional hypoxia induced BV2 cell model was established as a supplement to animal experiments to comprehensively understand the impact of YNFJ on the pathological and physiological processes of ischemic stroke and explore its molecular mechanisms. Our research suggested that YNFJ regulated NF- $\kappa$ B and Nrf2/HO-1 signaling pathways to inhibit oxidative stress damage and inflammatory damage after IS. However, we did not apply inhibitors to validate key regulatory proteins and pathways. Further studies are needed to select inhibitors and activators for key pathways for in-depth research. In addition, the nervous system is co-regulated by a variety of cells. This study only explored the regulatory effect of YNFJ on the two most widely distributed cells, microglia and neurons. More kinds of cells should be used in future research.

## 5. Conclusions

To sum up, network pharmacology demonstrated the underlying mechanism of YNFJ in the treatment of ischemic stroke. Topological feature analysis combined with enrichment analysis showed that, the mechanism of YNFJ in the treatment of ischemic stroke might be through the regulating of the NF- $\kappa$ B and Nrf2/HO-1 signaling pathway, in which IL6, TNF, PTGS2, NFKBIA and Nrf2 were indicated as the hub genes. Subsequently, experimental validation *in vitro* and *in vivo* provided convincing evidence that YNFJ ameliorated the inflammatory injury and oxidative stress injury of microglia caused by ischemic stroke by regulating NF- $\kappa$ B and Nrf2/HO-1 signaling pathway. In short, we provided new evidence for the development of YNFJ as a neuroprotective agent in the treatment of ischemic stroke.

## Funding statement

This work was supported by the National Natural Science Foundation of Jilin [No. YDZJ202201ZYTS279], the National Key Research and Development Program of China [2018YFC1706006 and 2019YFC1709902], the innovation and entrepreneurship training program for college students of Changchun University of Traditional Chinese Medicine [No. S202110199104].

## Data availability statement

Data included in article/supp. material/referenced in article.

## Ethics statement

This study was reviewed and approved by Experimental Animal Committee of Changchun University of Chinese Medicine, with the approval number: NO.2020143.

## CRediT authorship contribution statement

**Jing Lu:** Validation, Writing – original draft. **Xiaolei Tang:** Data curation, Formal analysis, Visualization. **Yuxin Zhang:** Data curation. **Hongbo Chu:** Investigation, Methodology. **Chenxu Jing:** Resources, Software. **Yufeng Wang:** Software. **Huijuan Lou:** Methodology. **Ziqi Zhu:** Formal analysis. **Daqing Zhao:** Funding acquisition. **Liwei Sun:** Writing – review & editing, Supervision. **Deyu Cong:** Supervision, Funding acquisition, Writing – review & editing.

## Declaration of competing interest

The authors declare that they have no known competing financial interests or personal relationships that could have appeared to influence the work reported in this paper.

## Appendix A. Supplementary data

Supplementary data to this article can be found online at <https://doi.org/10.1016/j.heliyon.2023.e23742>.

## References

- [1] J. Wang, Treatment of 36 cases of cerebral infarction with yinaofujian Capsule, China's Naturopathy 10 (2002) 38, <https://doi.org/10.19621/j.cnki.11-3555/r.2002.10.059>.
- [2] C. Ma, Study on the Curative Effect of Banxia Baizhu Tianma Decoction and Chuanhong Zhongfeng Capsule on Acute Cerebral Infarction (Wind Phlegm Blocking Collateral Syndrome), Changchun University of Traditional Chinese Medicine, Changchun, 2021, pp. 1–60, <https://doi.org/10.26980/d.cnki.gcczc.2021.000230>.
- [3] Y. Gao, Clinical Observation of Chuanhong Apoplexy Capsule on Convalescence of Cerebral Infarction (Blood Stasis Syndrome), Changchun University of Traditional Chinese Medicine, Changchun, 2020, pp. 1–46, <https://doi.org/10.26980/d.cnki.gcczc.2020.000105>.

- [4] X. Li, A Clinical Research in Acupuncture and Yi Nao Fu Jian Jiao Nang for a Stroke of Paralysis, Changchun University of Traditional Chinese Medicine, Changchun, 2018, pp. 1–32. <https://www.cnki.net>.
- [5] X.T. Jing Lu, Dongmei Zhang, Deyu Cong, Jian Wang, Effects of Yinao Fujian Formula on oxidative stress injury in MCAO rats and CoCl<sub>2</sub> induced PC12 cells, *China Journal of Traditional Chinese Medicine* 37 (2022) 5676–5681. <https://www.cnki.net>.
- [6] F. Jiao, K. Varghese, S. Wang, Y. Liu, H. Yu, G.W. Booz, R.J. Roman, R. Liu, F. Fan, Recent insights into the protective mechanisms of paeoniflorin in neurological, cardiovascular, and renal diseases, *J. Cardiovasc. Pharmacol.* 77 (2021) 728–734. <https://doi.org/10.1097/FJC.0000000000001021>.
- [7] X. Liu, Z. Mei, J. Qian, Y. Zeng, M. Wang, Puerarin partly counteracts the inflammatory response after cerebral ischemia/reperfusion via activating the cholinergic anti-inflammatory pathway, *Neural Regen Res* 8 (2013) 3203–3215. <https://doi.org/10.3969/j.issn.1673-5374.2013.34.004>.
- [8] Y. Liu, Z. Lian, H. Zhu, Y. Wang, S. Yu, T. Chen, J. Qu, J. Li, S. Ma, X. Chen, A systematic, integrated study on the neuroprotective effects of hydroxysafflor yellow A revealed by <sup>1</sup>H NMR-based metabolomics and the NF-kappaB pathway, *Evid Based Complement Alternat Med* 2013 (2013), 147362. <https://doi.org/10.1155/2013/147362>.
- [9] Y.J. Zhou, J.M. Chen, K. Sapkota, J.Y. Long, Y.J. Liao, J.J. Jiang, B.Y. Liang, J.B. Wei, Y. Zhou, Panax notoginseng saponins attenuate CCL2-induced cognitive deficits in rats via anti-inflammation and anti-apoptosis effects that involve suppressing over-activation of NMDA receptors, *Biomed. Pharmacother.* 127 (2020), 110139. <https://doi.org/10.1016/j.biopha.2020.110139>.
- [10] J. Gu, J. Chen, N. Yang, X. Hou, J. Wang, X. Tan, L. Feng, X. Jia, Combination of Ligusticum chuanxiong and Radix Paeoniae ameliorate focal cerebral ischemic in MCAO rats via endoplasmic reticulum stress-dependent apoptotic signaling pathway, *J. Ethnopharmacol.* 187 (2016) 313–324. <https://doi.org/10.1016/j.jep.2016.04.024>.
- [11] J.W. Tian, F.H. Fu, W.L. Jiang, C.Y. Wang, F. Sun, T.P. Zhang, Protective effect of hydroxysafflor yellow A against rat cortex mitochondrial injuries induced by cerebral ischemia, *Yao Xue Xue Bao* 39 (2004) 774–777. <https://doi.org/10.16438/j.0513-4870.2004.10.002>.
- [12] Y. Zhao, J. Zheng, Y. Yu, L. Wang, Panax notoginseng saponins regulate macrophage polarization under hyperglycemic condition via NF-kappaB signaling pathway, *BioMed Res. Int.* 2018 (2018), 9239354. <https://doi.org/10.1155/2018/9239354>.
- [13] T.T. Luo, Y. Lu, S.K. Yan, X. Xiao, X.L. Rong, J. Guo, Network pharmacology in research of Chinese medicine formula: methodology, application and prospective, *Chin. J. Integr. Med.* 26 (2020) 72–80. <https://doi.org/10.1007/s11655-019-3064-0>.
- [14] N.P. Committee, Pharmacopoeia of People's Republic of China, Chemical Industry Press, Beijing, 2005. <https://www.chp.org.cn/#/index>.
- [15] J. Lu, Q. Huang, D. Zhang, T. Lan, Y. Zhang, X. Tang, P. Xu, D. Zhao, D. Cong, D. Zhao, L. Sun, X. Li, J. Wang, The protective effect of DiDang Tang against AlCl<sub>3</sub>-induced oxidative stress and apoptosis in PC12 cells through the activation of SIRT1-mediated Akt/Nrf2/HO-1 pathway, *Front. Pharmacol.* 11 (2020) 466. <https://doi.org/10.3389/fphar.2020.00466>.
- [16] L. Li, M. Chen, G. Li, R. Cai, Raddeanin A induced apoptosis of non-small cell lung cancer cells by promoting ROS-mediated STAT3 inactivation, *Tissue Cell* 71 (2021), 101577. <https://doi.org/10.1016/j.tice.2021.101577>.
- [17] Y. Li, J. Zhu, Y. Liu, X. Chen, S. Lei, L. Li, B. Jiang, L. Tan, S. Yu, Y. Zhao, Glycogen synthase kinase 3 beta influences injury following cerebral ischemia/reperfusion in rats, *Int. J. Biol. Sci.* 12 (2016) 518–531. <https://doi.org/10.7150/ijbs.13918>.
- [18] B. Feng, L. Meng, L. Luan, Z. Fang, P. Zhao, G. Zhao, Upregulation of extracellular vesicles-encapsulated miR-132 released from mesenchymal stem cells attenuates ischemic neuronal injury by inhibiting smad 2/c-jun pathway via Acvr2b suppression, *Front. Cell Dev. Biol.* 8 (2020), 568304. <https://doi.org/10.3389/fcell.2020.568304>.
- [19] R. Jiang, J. Liao, M.C. Yang, J. Deng, Y.X. Hu, P. Li, M.T. Li, Lidocaine mediates the progression of cerebral ischemia/reperfusion injury in rats via inhibiting the activation of NF-kappaB p65 and p38 MAPK, *Ann. Transl. Med.* 8 (2020) 548. <https://doi.org/10.21037/atm-20-3066>.
- [20] M. Wang, X. Liu, Y. Wu, Y. Wang, J. Cui, J. Sun, Y. Bai, M.F. Lang, MuicrRNA-122 protects against ischemic stroke by targeting Maf 1, *Exp. Ther. Med.* 21 (2021) 616. <https://doi.org/10.3892/etm.2021.10048>.
- [21] A. Parray, Y. Ma, M. Alam, N. Akhtar, A. Salam, F. Mir, S. Qadri, S.V. Pananchikkal, R. Priyanka, S. Kamran, I.R. Winship, A. Shuaib, An increase in AMPK/e-NOS signaling and attenuation of MMP-9 may contribute to remote ischemic preconditioning associated neuroprotection in rat model of focal ischemia, *Brain Res.* 1740 (2020), 146860. <https://doi.org/10.1016/j.brainres.2020.146860>.
- [22] S. Li, D. Wu, M. Cao, Z. Yu, M. Wu, Y. Liu, J. Zhou, S. Yan, J. Chen, M. Huang, J. Zhao, Effects of choline supplementation on liver biology, gut microbiota, and inflammation in *Helicobacter pylori*-infected mice, *Life Sci.* 259 (2020), 118200. <https://doi.org/10.1016/j.lfs.2020.118200>.
- [23] X. Liu, G. Wu, N. Tang, L. Li, C. Liu, F. Wang, S. Ke, Glymphatic drainage blocking aggravates brain edema, neuroinflammation via modulating TNF-alpha, IL-10, and AQP4 after intracerebral hemorrhage in rats, *Front. Cell Neurosci.* 15 (2021), 784154. <https://doi.org/10.3389/fncel.2021.784154>.
- [24] R. Siracusa, R. D'Amico, M. Cordaro, A.F. Peritore, T. Genovese, E. Gugliandolo, R. Crupi, D. Impellizzeri, S. Cuzzocrea, R. Fusco, R. Di Paola, The methyl ester of 2-cyano-3,12-dioxoleana-1,9-dien-28-oiic acid reduces endometrial lesions development by modulating the NFkB and Nrf2 pathways, *Int. J. Mol. Sci.* 22 (2021). <https://doi.org/10.3390/ijms22083991>.
- [25] C. Guo, S. Wang, J. Duan, N. Jia, Y. Zhu, Y. Ding, Y. Guan, G. Wei, Y. Yin, M. Xi, A. Wen, Protocatechualdehyde protects against cerebral ischemia-reperfusion-induced oxidative injury via protein kinase cepsilon/nrf2/HO-1 pathway, *Mol. Neurobiol.* 54 (2017) 833–845. <https://doi.org/10.1007/s12035-016-9690-z>.
- [26] A. Tuttolomondo, M. Daidone, A. Pinto, Endothelial dysfunction and inflammation in ischemic stroke pathogenesis, *Curr. Pharmaceut. Des.* 26 (2020) 4209–4219. <https://doi.org/10.2174/1381612826666200417154126>.
- [27] A.D. Greenhalgh, S. David, F.C. Bennett, Immune cell regulation of glia during CNS injury and disease, *Nat. Rev. Neurosci.* 21 (2020) 139–152. <https://doi.org/10.1038/s41583-020-0263-9>.
- [28] A. Loboda, M. Damulewicz, E. Pyza, A. Jozkowicz, J. Dulak, Role of Nrf2/HO-1 system in development, oxidative stress response and diseases: an evolutionarily conserved mechanism, *Cell. Mol. Life Sci.* 73 (2016) 3221–3247. <https://doi.org/10.1007/s00018-016-2223-0>.
- [29] X. Wang, Z.Y. Wang, J.H. Zheng, S. Li, TCM network pharmacology: a new trend towards combining computational, experimental and clinical approaches, *Chin. J. Nat. Med.* 19 (2021) 1–11. [https://doi.org/10.1016/S1875-5364\(21\)60001-8](https://doi.org/10.1016/S1875-5364(21)60001-8).
- [30] A. Tuttolomondo, D. Di Raimondo, R. Pecoraro, V. Arnao, A. Pinto, G. Licata, Inflammation in ischemic stroke subtypes, *Curr. Pharmaceut. Des.* 18 (2012) 4289–4310. <https://doi.org/10.2174/138161212802481200>.
- [31] B.H. Clausen, L. Lundberg, M. Yli-Karjanmaa, N.A. Martin, M. Svensson, M.Z. Alfsen, S.B. Flaeng, K. Lyngso, A. Boza-Serrano, H.H. Nielsen, P.B. Hansen, B. Finsen, T. Deierborg, Z. Illes, K.L. Lambertsen, Fumarate decreases edema volume and improves functional outcome after experimental stroke, *Exp. Neurol.* 295 (2017) 144–154. <https://doi.org/10.1016/j.expneurol.2017.06.011>.
- [32] E. McNeill, M.J. Crabtree, N. Sahgal, J. Patel, S. Chuaiphichai, A.J. Iqbal, A.B. Hale, D.R. Greaves, K.M. Channon, Regulation of iNOS function and cellular redox state by macrophage Gch1 reveals specific requirements for tetrahydrobiopterin in NRF2 activation, *Free Radic. Biol. Med.* 79 (2015) 206–216. <https://doi.org/10.1016/j.freeradbiomed.2014.10.575>.
- [33] E.H. Kobayashi, T. Suzuki, R. Funayama, T. Nagashima, M. Hayashi, H. Sekine, N. Tanaka, T. Moriguchi, H. Motohashi, K. Nakayama, M. Yamamoto, Nrf2 suppresses macrophage inflammatory response by blocking proinflammatory cytokine transcription, *Nat. Commun.* 7 (2016), 11624. <https://doi.org/10.1038/ncomms11624>.
- [34] T.C. Nichols, NF-kappaB and reperfusion injury, *Drug News Perspect.* 17 (2004) 99–104. <https://doi.org/10.1358/dnp.2004.17.2.829042>.
- [35] M.A. Yenari, H.S. Han, Influence of hypothermia on post-ischemic inflammation: role of nuclear factor kappa B (NFkappaB), *Neurochem. Int.* 49 (2006) 164–169. <https://doi.org/10.1016/j.neuint.2006.03.016>.
- [36] W.T. Sun, C.L.H. Yang, T.C.T. Or, D. Luo, J.C.B. Li, Ginsenoside Rb1 from Panax notoginseng suppressed TNF-alpha-Induced matrix metalloproteinase-9 via the suppression of double-strand RNA-dependent protein kinase (PKR)/NF-kappaB pathway, *Molecules* 27 (2022). <https://doi.org/10.3390/molecules27228050>.
- [37] J. Bai, J. Zhao, D. Cui, F. Wang, Y. Song, L. Cheng, K. Gao, J. Wang, L. Li, S. Li, Y. Jia, A. Wen, Protective effect of hydroxysafflor yellow A against acute kidney injury via the TLR4/NF-kappaB signaling pathway, *Sci. Rep.* 8 (2018) 9173. <https://doi.org/10.1038/s41598-018-27217-3>.
- [38] G. Kaur, S.J. Han, I. Yang, C. Crane, Microglia and central nervous system immunity, *Neurosurg. Clin.* 21 (2010) 43–51. <https://doi.org/10.1016/j.nec.2009.08.009>.

- [39] G.A. Kurian, R. Rajagopal, S. Vedantham, M. Rajesh, The role of oxidative stress in myocardial ischemia and reperfusion injury and remodeling: revisited, *Oxid. Med. Cell. Longev.* 2016 (2016), 1656450, <https://doi.org/10.1155/2016/1656450>.
- [40] W. Li, S. Yang, Targeting oxidative stress for the treatment of ischemic stroke: upstream and downstream therapeutic strategies, *Brain Circ* 2 (2016) 153–163, <https://doi.org/10.4103/2394-8108.195279>.
- [41] V.P. Nakka, A. Gusain, R. Raghbir, Endoplasmic reticulum stress plays critical role in brain damage after cerebral ischemia/reperfusion in rats, *Neurotox. Res.* 17 (2010) 189–202, <https://doi.org/10.1007/s12640-009-9110-5>.
- [42] S. Gao, X. Duan, X. Wang, D. Dong, D. Liu, X. Li, G. Sun, B. Li, Curcumin attenuates arsenic-induced hepatic injuries and oxidative stress in experimental mice through activation of Nrf2 pathway, promotion of arsenic methylation and urinary excretion, *Food Chem. Toxicol.* 59 (2013) 739–747, <https://doi.org/10.1016/j.fct.2013.07.032>.
- [43] F. Bi, Y. Zhang, W. Liu, K. Xie, Sinomenine activation of Nrf2 signaling prevents inflammation and cerebral injury in a mouse model of ischemic stroke, *Exp. Ther. Med.* 21 (2021) 647, <https://doi.org/10.3892/etm.2021.10079>.
- [44] L. Mao, J. Chen, K. Cheng, Z. Dou, J.D. Leavenworth, H. Yang, D. Xu, L. Luo, Nrf2-Dependent protective effect of paeoniflorin on alpha-naphthalene isothiocyanate-induced hepatic injury, *Am. J. Chin. Med.* 50 (2022) 1331–1348, <https://doi.org/10.1142/S0192415X22500562>.
- [45] D. Zhang, M. Li, Puerarin prevents cataract development and progression in diabetic rats through Nrf2/HO-1 signaling, *Mol. Med. Rep.* 20 (2019) 1017–1024, <https://doi.org/10.3892/mmr.2019.10320>.
- [46] T. Hu, G. Wei, M. Xi, J. Yan, X. Wu, Y. Wang, Y. Zhu, C. Wang, A. Wen, Synergistic cardioprotective effects of Danshensu and hydroxysafflor yellow A against myocardial ischemia-reperfusion injury are mediated through the Akt/Nrf2/HO-1 pathway, *Int. J. Mol. Med.* 38 (2016) 83–94, <https://doi.org/10.3892/ijmm.2016.2584>.
- [47] Y.W. Kwon, S.Y. Cheon, S.Y. Park, J. Song, J.H. Lee, Tryptanthrin suppresses the activation of the LPS-treated BV2 microglial cell line via Nrf2/HO-1 antioxidant signaling, *Front. Cell. Neurosci.* 11 (2017) 18, <https://doi.org/10.3389/fncel.2017.00018>.